ANALYSIS OF NATURALLY OCCURRING

RADIONUCLIDES IN FLY ASH AND GYPSUM SAMPLES

By

Angela R. Roper

Thesis

Submitted to the Faculty of the

Graduate School of Vanderbilt University

in partial fulfillment of the requirements

for the degree of

MASTER OF SCIENCE

In

Physics

August, 2012

Nashville, Tennessee

Approved

Professor Michael G. Stabin

Professor David S. Kosson

ACKNOWLEDGEMENTS

TABLE OF CONTENTS

`

LIST OF TABLES

LIST OF FIGURES

INTRODUCTION

Exposure to humans to natural radiation from cosmic rays and from soil is an everyday

occurrence.   In addition to those forms of radiation, radionuclides from building materials may

cause further exposures. The burning of coal is a significant element in the US energy budget;

Figure 1[*] shows the primary forms of energy production in the United States.
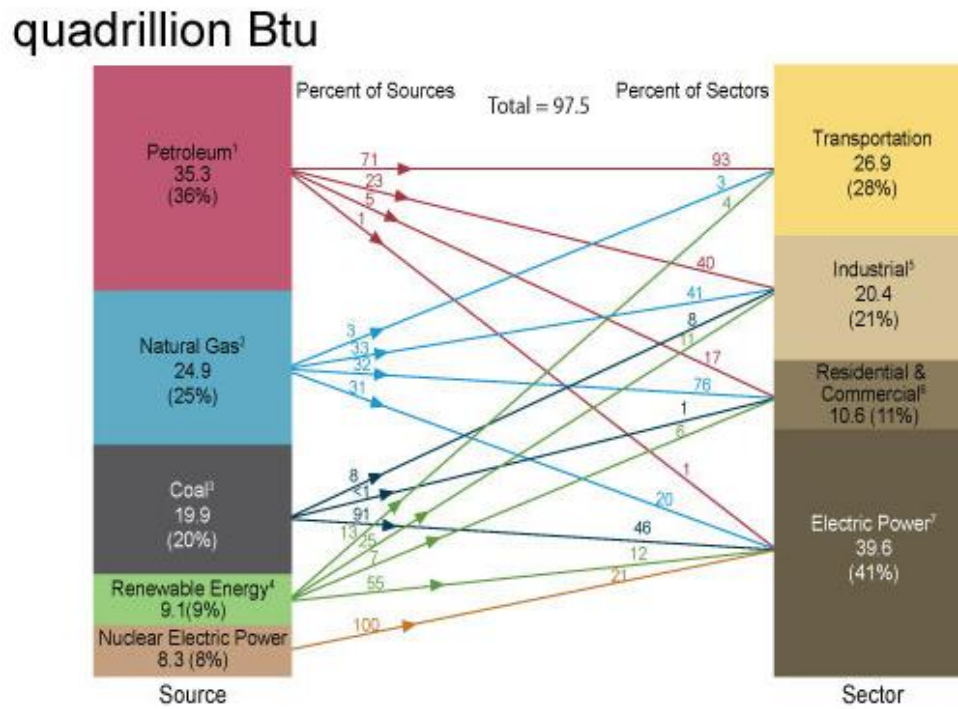
Figure 1. Energy production and usage in the United States.

_____

Coal fired power plants (CPPs) release naturally occurring radioactive material during the combustion of coal.   Fly ash, a by-product of CPPs, has many beneficial applications, for example in roads, building materials, concrete, cement and other materials.   From a survey from American Coal Ash Association (ACAA 2010) 6.77×10^7 short tons of fly ash were produced in 2010 and 2.57×10^7, 37.9%, was used beneficially, this percentage substantially greater than many countries (Baykal et al. 2011, Papastefanou 2010). Figure 2 shows results of a survey regarding fly ash use, along with other CCRs that can be used beneficially.

ACAA
15200 E. Girard Ave., Ste 3050
Aurora, CO 80014

Phone: 720-870-7897
Fax: 720-870-7889
Internet: www.ACAA-USA.org
Email: info@acaa-usa.org

2010 Coal Combustion Product (CCP) Production & Use Survey Report

Beneficial Utilization versus Production Totals (Short Tons)

CCP Categories	Fly Ash**	Bottom Ash**	Boiler Slag*	FGD Gypsum**	FGD Material Wet Scrubbers*	FGD Material Dry Scrubbers*	FGD Other*	FBC Ash*	CCP Production / Utilization Totals
2010 Total CCPs Produced by Category	67,700,000	17,800,000	2,332,944	22,000,000	8,670,814	1,405,952	3,740	10,267,914	130,181,364
2010 Total CCPs Used by Category	25,723,217	7,541,732	1,418,996	10,713,138	624,223	584,112	0	8,732,008	55,337,426
1. Concrete/Concrete Products /Grout	11,016,097	615,332	0	21,045		16,847	0	0	11,669,321
2. Blended Cement/ Raw Feed for Clinker	2,045,797	949,183	3,000	1,135,211		0	0	0	4,133,191
3. Flowable Fill	135,321	52,414	0	0		13,998	0	0	201,733
4. Structural Fills/Embankments	4,675,992	3,124,549	78,647	454,430	424,581	358,019	0	0	9,116,218
5. Road Base/Sub-base	242,952	715,357	3,128	0	3,018	0	0	0	964,455
6. Soil Modification/Stabilization	785,552	162,065	0	0		19,189	0	0	966,806
7. Snow and Ice Control	0	549,520	41,194	0		0	0	0	590,714
8. Blasting Grit/Roofing Granules	86,484	19,914	1,257,571	0		0	0	0	1,363,969
9. Mining Applications	2,399,837	528,881	0	835,536	186,624	112,373	0	8,660,408	12,723,659
10. Gypsum Panel Products	109	0	0	7,661,527		0	0	0	7,661,636
11. Waste Stabilization/Solidification	3,258,825	41,233	0	0		39,283	0	71,600	3,410,941
12. Agriculture	22,220	4,674	0	481,827		0	0	0	508,721
13. Aggregate	6,726	555,031	27,155	0		0	0	0	588,912
14. Miscellaneous/Other	1,047,305	223,579	8,301	123,562	10,000	24,403	0	0	1,437,150

Summary Utilization to Production Rate

CCP Categories	Fly Ash	Bottom Ash	Boiler Slag	FGD Gypsum	FGD Material Wet Scrubbers	FGD Material Dry Scrubbers	FGD Other	FBC Ash	CCP Utilization Total**
2010 Totals by CCP Type/Application	25,723,217	7,541,732	1,418,996	10,713,138	624,223	584,112	0	8,732,008	66,337,426
Category Use to Production Rate (%)***	37.90%	42.30%	60.80%	48.60%	7.10%	41.50%		85.00%	42.60%

2010 Cenospheres Sold (Pounds)	15,485,980	

ACAA received survey data representing 231,379 MegaWatts Name Plate capacity of the total industry-wide approximate 327,963 capacity (i.e., 69.7%) or approximately 67% of the coal-fueled electric utility generation as reported by EIA
* These are actual tonnages reported by utilities responding and do not reflect estimates for utilities that did not respond this year.
**These numbers are derived from previous, current and applicable industry-wide available data, including Energy Information Administration (EIA) Reports 923 and 860 and other outside sources.
***Utilization estimates are based on actual tons reported and on extrapolated estimates for fly ash, bottom ash, and FGD gypsum;

FINAL - 102011

Figure 2. 2010 Coal Combustion Product survey.

However, use of fly ash has come under scrutiny due to recent accidents, as well as a general interest in evaluating the possible dosimetric consequences for humans of use of this material in these applications. A notable fly ash spill occurred in Kingston, TN at a facility owned by the Tennessee Valley Authority (TVA) in 2008, in which over a billion gallons of fly ash and coal slurry were spilled due to a disposal cell rupture. This was the largest spill of this nature to occur in United States history. The Environmental Protection Agency (EPA) has thus decided to review their policies on regulation of fly ash. The EPA's proposal has two options, to regulate coal combustion residues (CCRs) under subtitle C as special wastes or under subtitle D as non-hazardous waste (40 CFR 75(118) 35128-35264); both options would operate under The Resource Conservation and Recovery Act (RCRA). Beneficial use of fly ash could be affected by this decision, though usage eliminates waste and saves money. Fly ash as an additive in concrete not only reduces the amount of waste products produced by CPPs but also increases the robustness of concrete by increasing the strength and durability of the concrete (Baykal and Saygili 2011).

In this work, analyses of the radioactive content of samples of fly ash were performed to determine if beneficial uses of fly ash in building materials could be of radiological concern. Analysis was also performed on samples of gypsum, scrubber sludge and fixated scrubber sludge. The content of ^{234}U and ^{232}Th decay series radionuclides, as well as of ^{40}K, was determined via gamma spectroscopy. Figures 2and 3 show the uranium chain and thorium decay series.
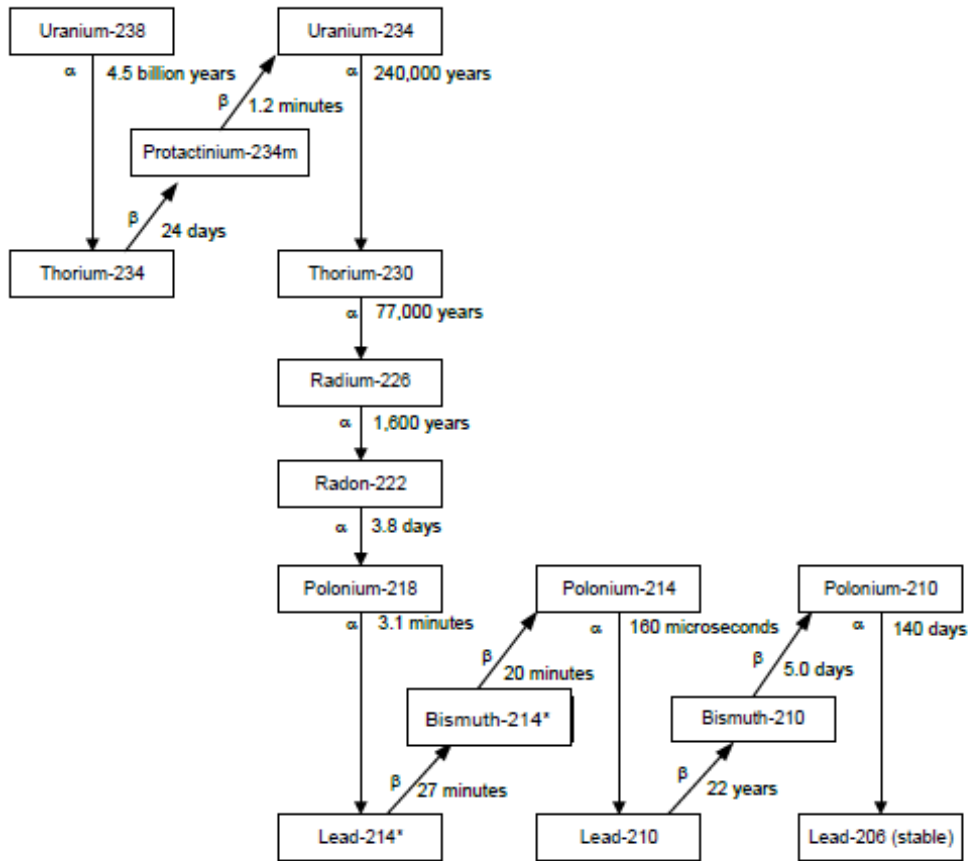
Figure 3. ^{238}Uranium decay series[†].
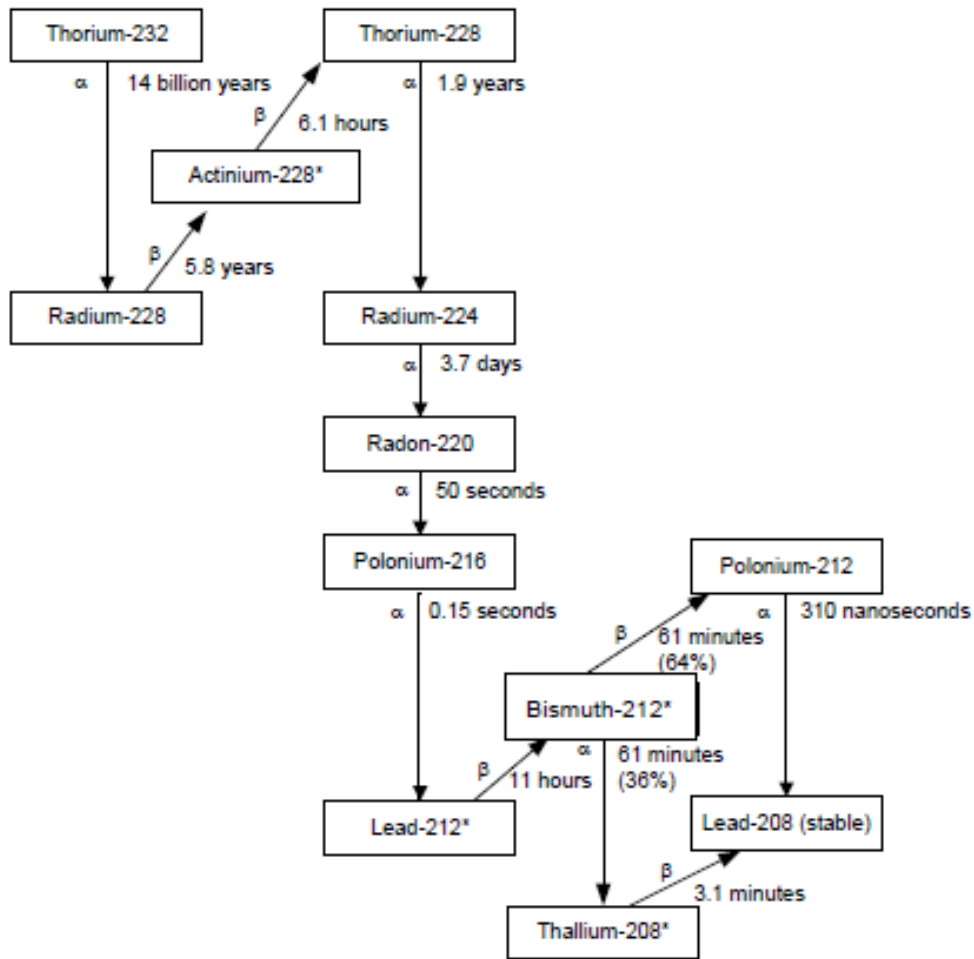
Figure 4. ^{232}Th decay series[‡].

^{40}K is not part of a decay series; it's 1461 keV gamma is the key gamma.
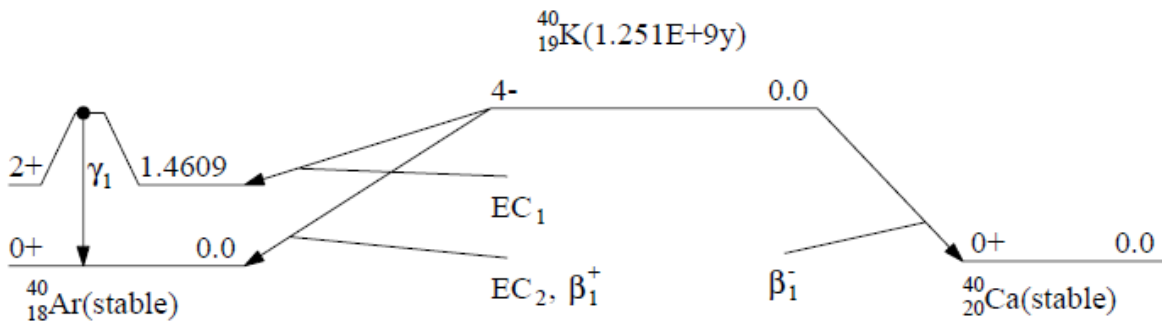
Figure 5. ^{40}K decay scheme.

After determination of typical fly ash radionuclide concentrations, a dosimetric analysis was performed using Monte Carlo transport simulations in concrete structures of various sizes assumed to contain different levels of incorporated fly ash.

CHAPTER II

LITERATURE REVIEW

Pathways to radiation dose

Radiation is ubiquitous; ionizing radiation from space constantly bombards our atmosphere and naturally occurring radionuclides are present in soil, water, food, air, and the human body. Radionuclides were produced when the universe first formed, although many have decayed away since their creation. Three important naturally occurring radionuclide decay chains – the uranium series, thorium series and actinium series, plus the radionuclide ^{40}K provide significant contributions to our external background radiation. ^{226}Ra, a daughter product of uranium, is responsible for the major fraction of internal dose, whether from ingestion or inhalation through ^{222}Rn gas. Uranium is present in soil and groundwater, which contribute to human exposures through internal and external exposure pathways.

When radiation was first discovered there was little understanding of the potentially deleterious effects of ionizing radiation to humans. Medical uses of x-rays and ^{226}Ra proliferated in the early 1900s, as the benefits of the medical uses of radiation began to be realized. But soon, short and long term effects of radiation were beginning to be understood. In 1925, Dr. A. Mutscheller suggested a limiting dose of 1/100 of a threshold erythema dose per month, an "R-unit." Simple limits of dose to the whole body to 1/10 of a 'skin erythema dose' per year, and an internal limit of 0.1 μg of radium in the body were proposed in 1941. Over subsequent decades, the international scientific community studied these effects extensively,

and dose limits were refined; finally in 1959 the ICRP released a report in the *Health Physics Journal* that laid the basis for a comprehensive system of radiation protection for radiation workers and the public. This work was mostly adopted and released as the first formal national US regulation of radiation exposures, Title 10 of the Code of Federal Regulations, Part 20, i.e. 10CFR20. (Stabin 2007).

Today, there are many laws regarding contamination from radiation exposure and inhalation, chemical toxicity, air pollution and water pollution. Throughout the 1950s and 1960s, a general realization grew in the US of the need to formalize a regulatory basis for protection of the environment from all forms of potential chemical and radiological damage, and this led to the formation of the Environmental Protection Agency (EPA) in 1970. In the recent years, nuclear regulations and policies have received heightened scrutiny because of the disaster at the Fukushima nuclear installation and debate over the high level waste (HLW) geologic repository in Yucca Mountain, Nevada. Some of the major laws regulating nuclear materials and waste are listed below (Clarke 2012)

- Atomic Energy Act of 1946 (McMahon Bill)
- Atomic Energy Act of 1954
- Energy Reorganization Act (1974)
- Uranium Mill Tailings Radiation Control Act (1978)
- Low Level Waste Policy Act (1980)
- Nuclear Waste Policy Act (1983)
- Low-Level Radioactive Waste Policy Amendments Act (1985)
- Nuclear Waste Policy Act As Amended (1987)
- Federal Facilities Compliance Act (1992)
- The Waste Isolation Pilot Plant Land Withdrawal Act (1992, 1996)

One of the most important regulations is the Atomic Energy Act (AEA) of 1954. It is the law that governs nuclear materials and waste, and both the Nuclear Regulatory Commission (NRC) and the EPA draw their enforcement jurisdiction from this act. The Nuclear Waste Policy Act (NWPA) of 1983 was established to develop a geologic repository for high level wastes (HLW) from the operation of nuclear power plants. The act authorized the creating of a repository, which after much study and expenditure of federal funds was determined to be in Yucca Mountain, Nevada. Due to political reasons, use of this site, as of this writing, has been put on hold indefinitely.

The EPA also established laws relating to environmental contamination such as the Safe Drinking Water Act (SDWA) and the Clean Air Act (CAA), which set limits of permissible levels of contaminates, both radioactive and chemical. The EPA also oversees implementation of the RCRA, which covers solid and hazardous waste. RCRA is important to this study because this is the act that will govern fly ash disposal, either under Subtitle C as hazardous waste or under Subtitle D as "special waste." However, currently, and perhaps in the future, fly ash is exempted from RCRA under the Bevell Amendment. When regulating hazardous materials, the EPA considers all avenues of contamination and the best analysis of possible receptors is to build a site conceptual model as in Figure 6 (Brown 2008).

Conceptual Burial Site Model
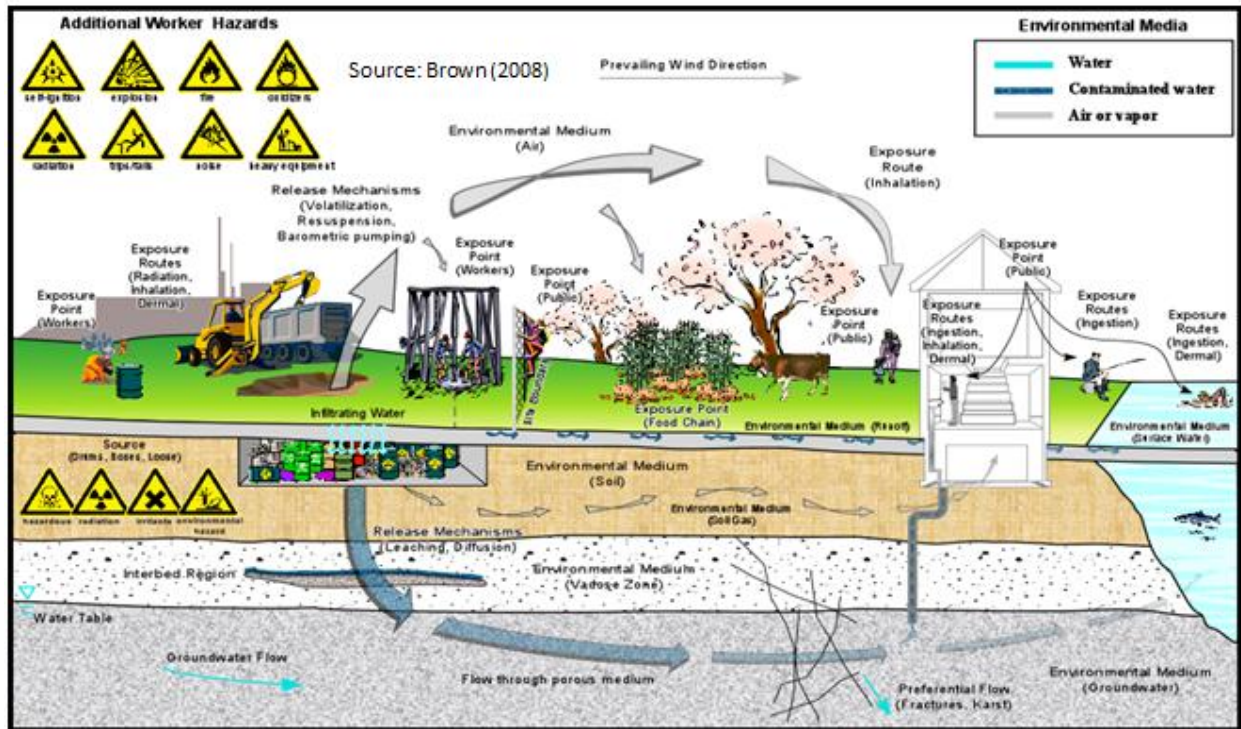
Figure 6. Conceptual site model with groundwater contamination pathway.

When overseeing the release of contaminates, such as the fly ash spill in Tennessee in 2008, the EPA uses such conceptual site models to determine the type of effect releases of this kind could have on the air, water, biota and many other factors.

Since the EPA, NRC and other regulatory bodies have been overseeing releases of radioactive materials to the environment, there have been areas found that have elevated concentrations of some radionuclides. For those that live in those areas, depending on the method of contamination, there are ways to circumvent this problem. For example, water supplies in the Atlantic coastal plain areas and piedmont provinces were found to exceed the existing radium limit of 185 Bqm^{-3} (5 pCiL^{-1}) (Lucas 1982, EPA 1991) with a maximum of 958

Bqm^{-3} (Hess 1985 et al.). A study was performed to determine the most effective water treatment method. Reverse osmosis and sodium ion-exchange processes were 92% effective and lime-soda ash softening processes reduced concentrations from 75 to 95% (Brinck et al. 1978).

Areas with high indoor radon have been discovered, e.g. the now famous Watras house in Pennsylvania. Mr. Watras worked at a nuclear power plant and set off radiation monitors consistently. It was determined that the radiation was of natural origin, and the Watras home was tested for ^{222}Rn; the indoor radon concentration was found to be 100 kBq m^{-3} (2700 pCi L^{-1}). The Watras were advised to vacate the premises by the Pennsylvania Department of Energy Resources. This event has widely been seen as the triggering point that led to the Indoor Abatement Act, which led to research of indoor radon concentrations (Cole 1993).

Fortunately, there are ways to reduce exposures to radon gas. A simple way is to use air filtration systems or fans throughout the home to increase air turnover (Curling et al. 1990a,b). One may seal openings in the foundations of the home or use "sub-slab suction" devices to draw out the gas (Eisenbud and Gesell 1997). It is important to note that while exposure to high levels of radon may be potentially dangerous, most levels are low and if higher concentrations can be managed with the abatement methods described above. Risk informed regulations should be implemented, so as to balance cost and benefit (Clarke 2012).

All building materials contain radionuclides at some levels Using fly ash in concrete, increases the durability of the concrete, reduces the need to utilize natural resources and it eliminates costly waste, but may raise the dose from naturally occurring radionuclides present in the coal combustion residues.

Inhalation of radon gas is one of two pathways humans can receive a radiation dose from fly ash within building materials, the second being external dose by gamma rays. Fly ash contains radionuclides from the uranium series, thorium series and ^{40}K. These nuclides emit alpha, beta and gamma radiation. While alpha and beta radiation are particles will be absorbed within the walls, gamma radiation is an electromagnetic wave and can penetrate through the walls. However, both the uranium and thorium series have radon isotopes; radon is a noble gas, and so can diffuse out of the concrete. It and its progeny emit alpha, beta and gamma radiation. The dose one receives depends on the porosity of the concrete, the air exchange rate in the room, the occupancy, distance and percentage of the concrete/fly ash mixture. The radon itself is inhaled and exhaled quickly, but the progeny are usually attached to dust particles, due to their electrostatic charge, and may be deposited on the walls of the respiratory tract and deliver dose to important tissues there over their longer retention time (Eisenbud 1997).

A study from the US Geological Survey (USGS 1997) concluded that the majority of our radiation exposure comes from natural sources.
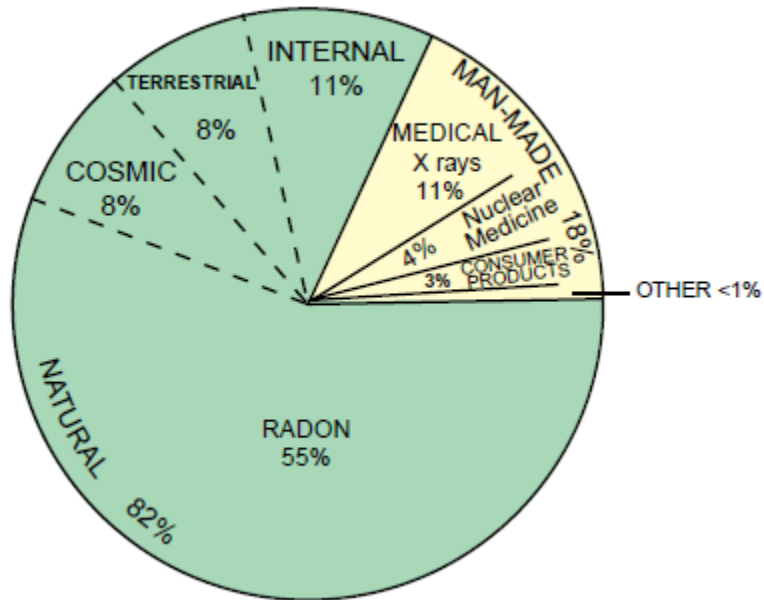
Figure 7. US Geological Survey for natural radiation.

Most of the radiation dose we receive actually comes from natural sources – natural radon, cosmic radiation and terrestrial from the soil.   Furthermore, all building materials are radioactive to some extent, whether from natural or artificial origin.

Literature on specific activity of fly ash and other pertaining material

There are conflicting views as to whether use of fly ash could represent a significant risk to human health. A study from the European Commission (EC 112) found that there was potential to have annual exposures above 1 mSv in buildings with concrete containing a high

percentage of fly ash and possible if the use natural building stones are used in bulk amounts.

They defined an 'activity concentration index' (I) for identifying whether a dose criterion is met

using the following formula:

$$I = \frac{C_{Ra}}{300 \ Bq \ kg^{-1}} + \frac{C_{Th}}{200 \ Bq \ kg^{-1}} + \frac{C_K}{3000 \ Bq \ kg^{-1}}$$

Where C_{Ra}, C_{Th}, C_K is the specific activity of ^{226}R, ^{232}Th, ^{40}K. The activity concentration index

should not exceed the following values below depending on the dose criterion and the way and

the amount the material is used in a building.

Dose criterion	0.3 mSv a^{-1}	1 mSv a^{-1}
Materials used in bulk amounts, e.g. concrete	I ≤ 0.5	I ≤ 1
Superficial and other materials with restricted use: tiles, boards, etc.	I ≤ 2	I ≤ 6

The study also found one could get an annual effective dose of about 0.25 mSv in addition to

the dose received outdoors living in an apartment block made of concrete with average

concentrations of 40, 30, and 400 Bq kg^{-1} for radium, thorium and potassium respectively

(Markkanen 1995).

The most common method to determine the specific activity of these materials is

gamma ray spectroscopy using HPGe (El Afifi et al. 2006), but other methods may be used, such

as alpha particle spectrometry, beta particle counting or gamma measurements after

radiochemical separation (Johnston 1997, Koler 2002). Also, it has been pointed out that radon

isotopes may not necessarily be in secular equilibrium with parent nuclides due to geo-chemical

processes (Kovler et al. 2005).

Specific activities for fly ash, building materials and other sources have been given in

Tables 2-9. Turhan et al. (2010) evaluated fly ash concentrations of ^{238}U[§], ^{232}Th, and ^{40}K and

found values between 17 to 2720, 9 to 696, 12 to 2974 Bq kg^{-1}, respectively. This is a

considerable range, and many of the literature values have wide a wide range. Coles et al.

(1978), in a domestic study, the range was decreased and found lower overall maximum

concentrations, with ^{238}U, ^{232}Th, and ^{40}K values between 70 to 130, 63 to 89, 233 to 300 Bq kg^{-1},

respectively. Similar results were given in a European Commission study (EC 112 1999), which

showed a much higher range of concentrations, with means of 180, 100, 650 Bq kg^{-1} for ^{238}U,

^{232}Th, and ^{40}K. Other studies have found concentrations of 117.5, 126.8, 687 and 134.2, 74.7,

646.9 Bq kg^{-1} for ^{238}U, ^{232}Th, and ^{40}K (Nakaoka et al. 1984, Bem et al. 2002). Literature values

for natural gypsum have average means of 15, 13.6, 112 for ^{238}U, ^{232}Th, and ^{40}K (EC 112 1999,

Trevisi et al. 2012, El Afifi et al. 2006, NCRP 1987).

The specific activity in uranium and radium is related inversely to the diameter of the

ash. Also, fly ash size varies depending on the stage within the coal fired power plant;

Papastefanou (2010) took fly ash from three separate stages in the combustion process and

found as the ash flows towards the stack, they decrease in diameter, as seen from below.

[§] Assuming secular equilibrium with ^{226}Ra and ^{238}U
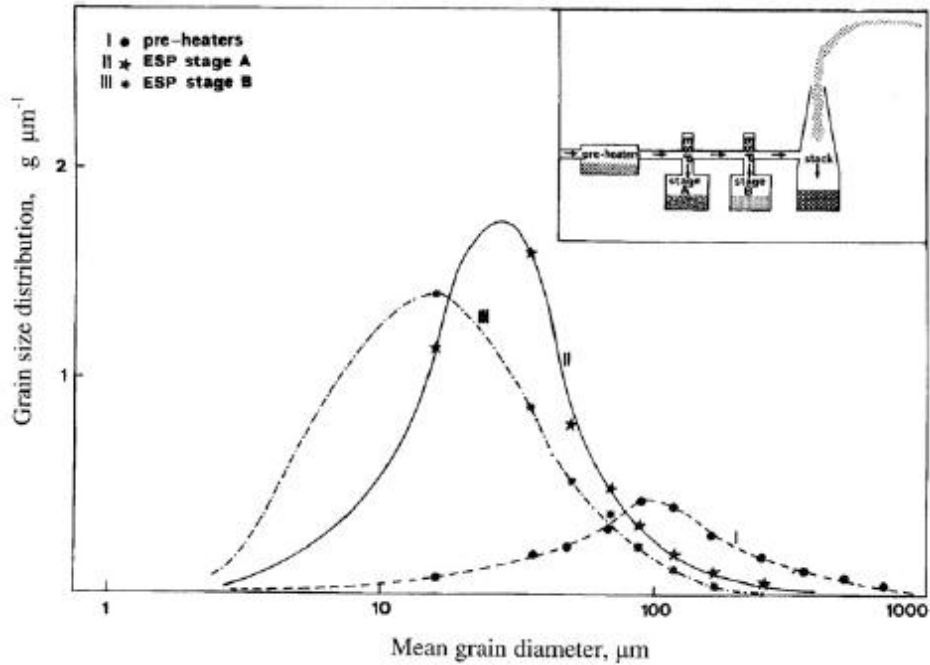
Figure 8. Mean diameter of ash throughout the combustion process.

Table 1. Specific activity throughout the combustion process.

Sampling location	^{238}U (Bq kg^{-1})	^{226}Ra (Bq kg^{-1})
Preheaters	340.4	192.4
ESP stage A	481.0	336.7
ESP stage B	640.1	499.5

The specific activities are seen to be different by as much as a factor of two depending on the

point in combustion.

16

Table 2. Fly ash concentrations reported by other investigators (Bq kg^{-1}).

	^{238}U			^{232}Th			^{40}K			Source
	Mean	Min	Max	Mean	Min	Max	Mean	Min	Max	
				100		300	650		1500	EC 112 (1999)
	356	263	950				297	204	382	Papastefanou (2010)
	574	460	870							Papastefanou et al. (1979)
				102	9	696	517	12	2974	Turhan et al. (2010)
	97	44	169	74	33	126	728	185	1547	Tomczynska et al. (1980)
				132	107	207	268	56	348	Mirshra et al. (1984)
	118	106	124	127	114	13	687	618	722	Nakaoka et al. (1984)
	89	76	114	91	57	130	364	170	615	Fardy et al. (1989)
				111	90	126				Hayumbu et al. (1995)
	134	94	185	75	48	92	647	449	758	Bem et al. (2002)
		70	130		63	89		233	300	Coles et al. (1978)
Mean	228	159	363	101	65	198	520	241	1016	
Standard deviation	197	151	375	22	37	203	186	200	868	
Min	89	44	114	74	9	13	268	12	300	
Max	574	460	950	132	114	696	728	618	2974	

Coal, like fly ash, can be highly variable in radionuclide concentration. One study found the specific activity of uranium to be as high as 15,000 Bq kg^{-1} in coal from Freital, Germany (Vandenhove 2000). Others have found 1,480 Bq kg^{-1} of ^{226}Ra in coal samples from Illinois and 2,590 Bq kg^{-1} of ^{226}Ra in coal from Northern Greece (Barber and Giorgio 1977, Papastefanou and Charalambous, 1979, 1980).

Secular equilibrium between [238]U and [226]Ra in fly ash has been contested by many

(Kovler et al. 2005, Papastefanou and Charalambous, 1979, 1980) but it is usually assumed for

coal (Coles et al. 1978). One study hypothesized an surplus of [238]U due to precipitation in

reduction zones in coal mines or removal of [234]U by flowing waters (Papastefanou 2010).

Table 3. Coal concentrations reported by other investigators (Bq kg^{-1}).

	[238]U			[232]Th			[40]K			Source
	Mean	Min	Max	Mean	Min	Max	Mean	Min	Max	
	18	1	540	21	2	320	52	1	710	Beck, DOE - 1980
		9	32		6	21		27	52	Coles et al.(1978 - US)
	385	298	435							Papastefanou et al. (1979)
	38	2	141	30	9	107	294	37	759	Tomczynska et al. (1980)
				37	26	48	95	7	200	Mishra et al. (1984)
	12	6	16	13	7	19	72	40	180	Nakaoka et al. (1984)
	24	13	39	14	9	153				Bem et al. (2002)
	243	117	399				108	59	227	Papastefanou (2010)
	12			8			26			Tracy et al. (1985)
	416						106			Font et al. (1993)
Mean	144	64	229	20	10	111	108	29	355	
Stdev	177	111	222	11	8	115	87	22	301	
Min	12	1	16	8	2	19	26	1	52	
Max	416	298	540	37	26	320	294	59	759	

World average building material specific activity has been cited to be 50, 50, and 500 Bq

kg^{-1}, with world average soil levels of 35 (17-60), 30 (11-64), 400 (140-850) Bq kg^{-1} for [226]Ra,

[232]Th, and [40]K respectively (UNSCEAR 1993, UNSCEAR 2000). Radiation exposures from

radionuclides in building materials depend on the type of materials used; wood for example, does not have much radioactivity but it shields less from cosmic radiation. Soil concentrations can be highly variable, with levels reported as high as 1,000 Bq kg^{-1} for ^{238}U, 360 Bq kg^{-1} for ^{232}Th and 3,200 Bq kg^{-1} for ^{40}K (UNSCEAR 2008).

Table 4. Cement concentrations reported by other investigators (Bq kg^{-1}).

	^{238}U			^{232}Th			^{40}K			Source
	Mean	Min	Max	Mean	Min	Max	Mean	Min	Max	
	18			14			293			Ramadan et al. (2006)
				48			115			Beretka et al. (1985)
				59			564			Malancea et al. (1993)
				29			273			Khan et al. (2001)
				24			432			Kumar et al. (1999)
				27			422			Amrani et al. (2001)
	51			23			832			Ibrahim (1999)
				19			230			Ackers et al. (1985)
				132			506			Mollah et al. (1986)
				37			173			Xinwei (2005)
	46			21			237			NCRP (1987)
Mean	38			39			371			
Stdev	18			34			208			
Min	18			14			115			
Max	51			132			832			

Table 5. Concrete concentrations reported by other investigators (Bq kg^{-1}).

	^{238}U			^{232}Th			^{40}K			Source
	Mean	Min	Max	Mean	Min	Max	Mean	Min	Max	
				30		190	400		1600	EC 112 (1999)
				40		190	430		1600	EC 112 (1999)
				37	12	65	354	95	766	Ademola (2005)
				35	1	152	392	7	1450	Trevisi (2012)
Limestone	31			9			89			NCRP (1987)
Sandstone	1			9			385			NCRP (1987)
		19	89		15	120		260	1100	(Eicholz, 1980)
Mean	16	30	435	27	16	133	342	163	1269	
Stdev	21	16	489	14	15	54	126	135	335	
Min	1	19	89	9	1	65	89	7	766	
Max	31	41	780	40	37	190	430	290	1600	

Table 6. Soil concentrations reported by other investigators (Bq kg^{-1}).

	^{238}U			^{232}Th			^{40}K			Source
	Mean	Min	Max	Mean	Min	Max	Mean	Min	Max	
US	35	4	140	35	4	130	370	100	700	UNSCEAR(2000)
World	33			45			420			UNSCEAR (2000)
	22			37			400			NCRP(1987)
				34	1	258	483	0	3200	UNSCEAR (2010)
Mean	30	4	140	38	3	194	418	50	1950	
Stdev	7	----	----	5	2	91	48	71	1768	
Min	22	4	140	34	1	130	370	0	700	
Max	35	4	140	45	4	258	483	100	3200	

Table 7. Natural gypsum concentrations reported by other investigators (Bq kg^{-1}).

	^{238}U			^{232}Th			^{40}K			Source
	Mean	Min	Max	Mean	Min	Max	Mean	Min	Max	
				10			80			EC 112 (1999)
						100			200	Mustonen (1997)
				9	1	100	91	5	279	Trevisi et al. (2012)
				28	25	30	129	126	132	El Afifi et al. (2006)
	15			7			148			NCRP (1987)
Mean	15	----	-----	14	13	77	112	66	204	
Stdev	----	----	----	10	17	40	32	86	74	
Min	15	----	----	7	1	30	80	5	132	
Max	15	----	----	28	25	100	148	126	279	

Table 8. Brick concentrations reported by other investigators (Bq kg^{-1}).

	^{238}U			^{232}Th			^{40}K			Source
	Mean	Min	Max	Mean	Min	Max	Mean	Min	Max	
Clay (red)				50		200	670		2000	EC 112 (1999)
Sand-lime				10		310	640		4000	EC 112 (1999)
		4	180		1	140		7	1200	Eicholz (1980)
Range				48	2	164	598	12	1169	Trevisi (2012)
Clay	111			11						NCRP (1987)
		4	180		1	140		7	1200	Eicholz (1980)
Mean	111	4	180	30	1	191	636	9	1914	
Stdev	----	0	0	22	1	71	36	3	1218	
Min	111	4	180	10	1	140	598	7	1169	
Max	111	4	180	50	2	310	670	12	4000	

Table 9. Stone and rock concentrations reported by other investigators (Bq kg^{-1}).

	^{238}U			^{232}Th			^{40}K			Source
	Mean	Min	Max	Mean	Min	Max	Mean	Min	Max	
				60			640			EC 112 (1999 - Europe)
					310				4000	Mustonen et. al (1997)
Igneous	48			48			810			UNSCEAR (1958)
Sandstone	15			24			330			UNSCEAR (1958)
Shales	15			41			810			UNSCEAR (1958)
Limestone	15			5			81			UNSCEAR (1958)
Igneous - Basalt		7	10		10	15	300			NCRP (1987)
Igneous - Mafic	10			10				70	400	NCRP (1987)
Igneous - Salic	60			80				1100	1500	NCRP (1987)
Igneous - Granite	40			70				1000		NCRP (1987)
Shale sandstones	40			50			800			NCRP (1987)
Clean quartz			10			8			300	NCRP (1987)
Igneous plutonic				89	0	906	1049	24	2040	Trevisi et. al (2012)
Igneous volcanic				163	8	750	1295	170	2354	Trevisi et. al (2012)
Metamorphic				21	0	142	395	0	1891	Trevisi et. al (2012)
Granite				70	65	75	1560	1340	1780	El Afifi et. al (2006)
Mean	30	7	10	56	17	315	734	529	1783	
Stdev	19	----	0	42	27	367	449	589	1166	
Min	10	7	10	5	0	8	81	0	300	
Max	60	7	10	163	65	906	1560	1340	4000	

When fly ash is used as an additive in concrete, the increase of radionuclide

concentration is only about 3 percent in comparison to other building materials, such as red

brick, that contain higher natural concentrations of radionuclides (Eisenbud 1997). Direct

measurement of the increase in radon is difficult because radiation emanation from the soil

below the dwelling, which dominates the radon inhalation over building materials and other

sources (Eisenbud and Gesell 1997).   However is it is estimated that concrete of all types only

contribute less than 10 percent of the indoor radon dose (Eisenbud 1997). Of more concern

from CCRs might include the leaching of constituents like arsenic, selenium and lead into

groundwater but concentrations of these elements are variable from site to site (Eisenbud

1997).

Literature on ^{222}Rn internal dose

Addition of fly ash to concrete may have an effect on the radon exhalation rate, but

surprisingly there are several literature sources that claim that it has no effect (Ulbak et al.

1984, Van Dijk et al. 1991) and maybe even causes a reduction in the radon 'exhalation rate'

(Stranden, 1983, Ackers et al. 1985, Kovler et al. 2005). Others disagree and believe that the

addition of fly ash to concrete increases the radon exhalation rate (Siotis et al. 1984). Kolver et.

al 2005 calculated a typical dose due to ^{222}Rn to 0.227 mSv y^{-1}, assuming an 'emanation

coefficient', the fraction of radon that escape from a material, of 5%. Dose from ^{220}Rn was only 9.5

µSv y^{-1} for the same emanation coefficient, so doses from ^{220}Rn are low and are of very little

importance compared to that from ^{222}Rn. A study was done for emanation factors of 1,5,10

and 15 percent; dose from radon increased with increases in the emanation factor (Kolver et al.

2005). The final results showed a reduction in radon emanation due to the 0.52 percent

emanation coefficient of fly ash, compared to the 7.65 percent coefficient of Portland cement,

despite the fly ash being three times higher in [226]Ra content. The dose depends on the area in question as well, whereas this study was done with small rooms vs. larger volumes (Taylor-Lange et al. 2012). It is debatable which is the best emanation coefficient to be used, one study found the best number to use would be 5%, while another believed it should be given in a range of 2-5%, and another used a variety of different ones but believed the best to 5% as well (Siotis et al, 1984 Stranden 1983, Taylor-Lange et al. 2012).

Table 10. [222]Rn inhalation ($\mu Sv\ y^{-1}$) with varying emanation coefficients.

Description	$\mu Sv\ y^{-1}$ due to [222]Rn inhalation	Source
No fly ash	< 54	Taylor-Lange et. al 2012
25% fly ash,5% emanation	95	Taylor-Lange et. al 2012
1% emanation	44	Kolver et. al 2005
5% emanation	227	Kolver et. al 2005
10% emanation	455	Kolver et. al 2005

Gamma spectroscopy

For this experiment two p-type coaxial high purity germanium detectors (HPGe) were used for gamma counting. The detectors have a P-I-N structure, which means there in an Intrinsic (I) region is sensitive to the ionizing radiation from the X-rays and gamma rays. When under a reverse bias, an electric field extends across the depleted region, also known as the intrinsic region. When photons interact within the depleted region charge carriers, namely holes and electrons, are produced and are swept away by the electric field to the P and N electrodes. This charge is proportional to the energy deposited by the photon and it is

converted into a voltage pulse by an integral charge-sensitive preamplifier. The process is

illustrated in Figure 9[**].
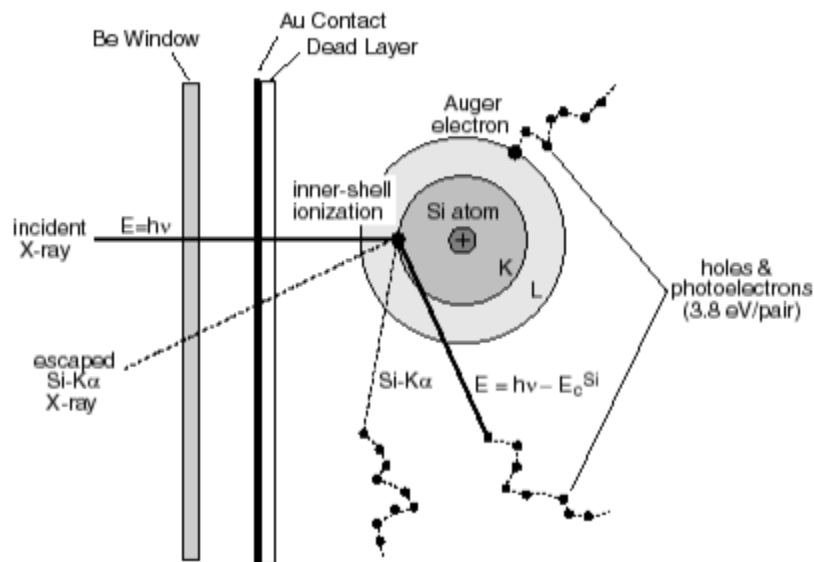
Figure 9. Electron-hole pair production.

These detectors have a low band gap and must be cooled by liquid nitrogen to reduce the

reverse leakage current to an acceptable level; otherwise noise destroys the energy resolution.

Coaxial HPGe detectors have a high efficiency, high resolution and it takes little energy (~1.1 eV)

to produce charge carriers, which makes it perfect for the current study (Canberra 1998).

Figure 10 shows a diagram of a typical Canberra HPGe detector[††].
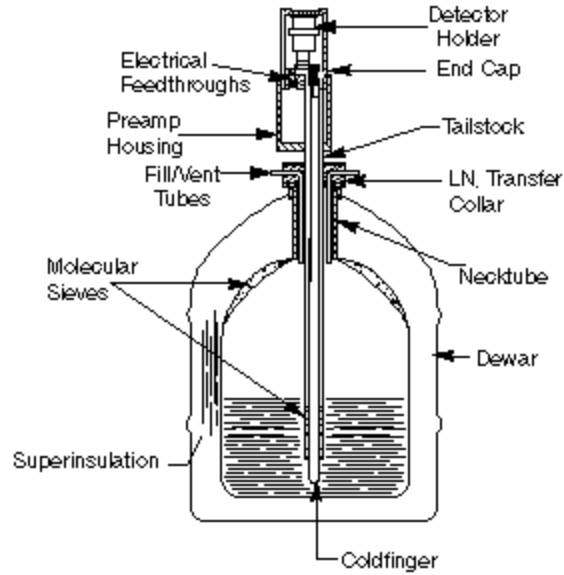
Figure 10. Canberra HPGe detector.

In any radiation counting, one must understand the counting system's detection limits; with samples containing environmental levels of radioactivity, concentrations often may be close to detection limits. The key quantity determining detectability is the Lower Limit of Detection (LLD) (Currie 1968). Expressed mathematically this is:

$$LLD = 4.66\sigma + 2.71$$

where $\sigma = \sqrt{N_B}$, with N_B being the number of background counts

LLD is defined as the counts above background that can be seen with a 5% chance of making a Type I or Type II error. A type I error is an error in which a background count is called a positive count, and a Type II error is an error in which a positive count is called a background count. The Minimum Detectible Activity (MDA) is the lowest level of activity that can be seen at the LLD. The equation for MDA is (Currie 1968, Knoll 2000):

26

$$MDA = \frac{4.65\sigma_B + 2.71}{f\epsilon T}$$

where f = radiation yield per disintegration
ϵ = absolute detection efficiency
T = counting time

Currie (1968) goes on to define three regions in which the analyst's confidence can be defined.

1. L_C (critical level) – the activity is different from zero with 95% confidence. $L_C = 2.33\sigma_B$

2. L_D (detection level) – also known as the MDA, smallest true signal that can be detected, it keeps the Type I and II errors to 5%.

3. L_Q (determination level) – the true value of the net signal has a relative standard deviation of 10%. Mathematically it is

$$L_Q = 50\left\{1 + \left[1 + \frac{\sigma_B}{12.5}\right]^{1/2}\right\}$$

Currie really recommended that quantitative assessment be done only above L_Q, however, the majority of health physicists are comfortable reporting values above L_D (the MDA), and for this study MDAs were used to define the limit at which numerical values were reported (Currie 1968, Stabin 2000). One can extend this to be a minimum detectible activity concentration (Bq kg^{-1}) by dividing by the sample mass.

In gamma spectrometry, one must look at the spectrum of detected photons and determine the origin of the peaks. An example spectrum can be seen below[‡‡].

[‡‡] http://www.pas.rochester.edu/~AdvLab/6-Gamma/Lab06%20GammaSp.pdf
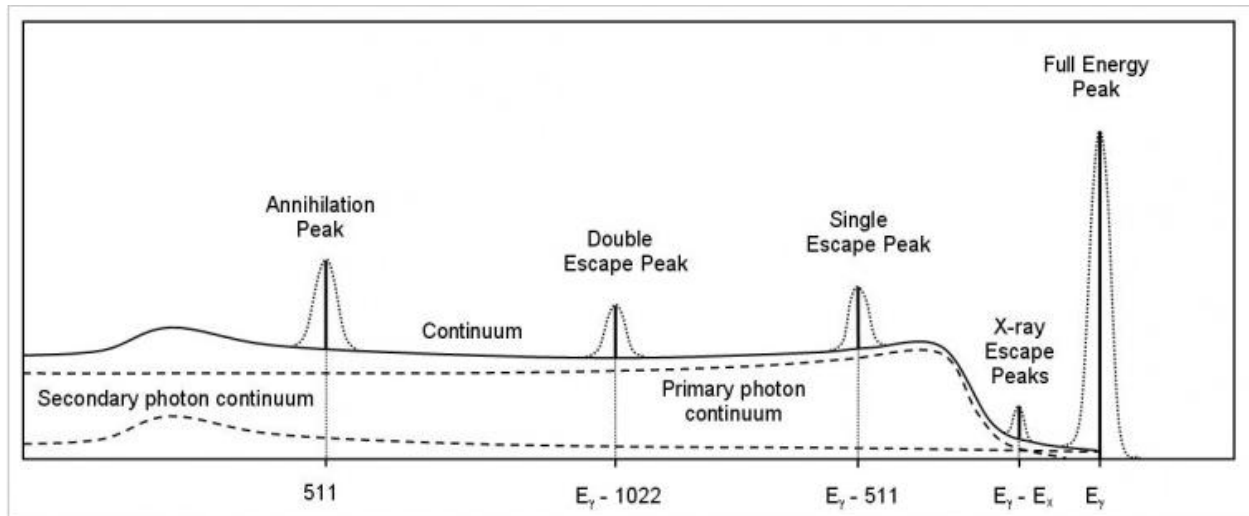
Figure 11. Typical gamma spectrum.

The spectrum shows the gamma photopeaks of a typical radionuclide, as well as all the interactions, including scattering events and other photopeaks. The three main photon interactions of interest are photoelectric scattering, Compton scattering, and pair production. When a photoelectric event occurs, the photon energy is completely absorbed, and the energy event is shown as an event from a photon of this energy ('full energy' event in the diagram above). Compton scattering occurs when a photon interacts with an orbital electron, the photon is scattered in another direction and loses energy. The orbital electron is ejected from the atom with the energy lost from the photon. The Compton equation is given as:[§§]

[§§] http://hyperphysics.phy-astr.gsu.edu/hbase/quantum/compton.html
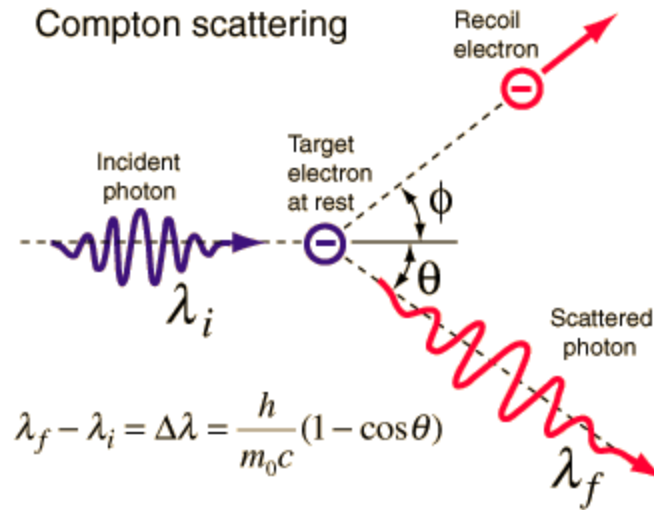
Figure 12. Compton scattering.

To get the equation in terms of energy we use

$$E = h\nu = \frac{hc}{\lambda}$$

where h = Planck's constant, $6.63*10^{-34}$ J-s
ν = frequency of the electromagnetic radiation s^{-1}
λ = wavelength [m]
c = speed of light, $3*10^8$ ms^{-1}

$$E' = \frac{E}{1 + \dfrac{E/m_0 c^2}{1 - cos\theta}}$$

where m_o = the electron rest mass

Any and all scattering angles may occur in a given scattering event. Thus, a 'continuum' of

partial energy events will be shown in the spectrum (Figure 11, above) on which full photopeak

events are superimposed, representing partial photon deposition in the detector. However, if

one or more Compton events occur in the detector followed by a photoelectric event, all of this

energy will be scored within the detector event resolution time and will represent a full

photopeak event. If the photon energy is above 1.02 MeV, pair production events are possible.

In pair production, one or both of the 511 keV photons may be detected. If one is detected and

the other escapes, a 'single escape peak' results; if both annihilation photons escape the

detector, a 'double escape peak' is recorded. When two full photopeak events are detected at

the same time, it is registered as a photopeak event at the sum of the two photon energies,

thus representing a false 'sum peak'. After eliminating false peaks in a spectrum, true

photopeak events of parent or progeny nulcides are used to confirm identification of the key

photopeaks of interest. With nuclides in a decay chain in secular equilibrium, the areas under

the various photopeaks will be theoretically equal, when properly weighted for photon

abundance and detector efficiency at each energy.

A typical efficiency plot of HPGe detector is shown in Figure 13.
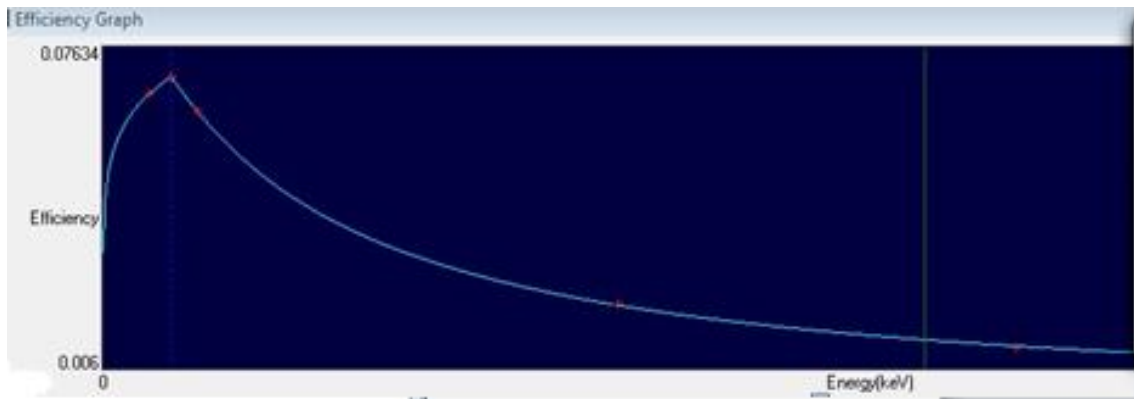
Figure 13. Efficiency plot of an HPGe detector.

The efficiency curve of a Ge detector consists initially of a quadratic function, then the tail turns

into a somewhat linear function, with the two being separated by a 'knee.'

Literature on Monte Carlo simulations

Monte Carlo simulation of radiation transport is a well-established and validated science.

Very simple codes can be written, for example to model photon attenuation in a uniform

medium. In most applications, however, the geometries and materials are complex, and

modeling of the transport of different types of radiation requires a complicated and well

validated code. Several of the widely available and used Monte Carlo codes are:

1. EGS4 (Ford and Nelson 1978) - electron gamma shower code, a general purpose code

   for coupled transport of electrons and photons in different geometries for particles with

   energies from a few keV to several TeV. Originally designed for modeling of radiation

   therapy, but it can be used in external, internal and detector dose calculations.

2. MCNP (Briesmeister 1997) – Monte Carlo N-particle transport code, can be used for

   neutron, photon, electron, or coupled neutron/photon/electron transport modeling in

   complicated three-dimensional geometries. Originally designed for modeling of reactor

   environments, but it can be used for external, internal, detector and many other dose

   calculations.

3. ALGAMP (Ryman and Eckerman 1993) – Organ doses are calculated by scoring energy

   deposition in all organs except skeletal tissues. It was the first to define all the original

   absorbed fractions, and it was used for years in internal dosimetry. It was not

   distributed widely, being mostly used within Oak Ridge National Laboratory in Oak

Ridge, TN, but it was used for many years to determine tables of absorbed fractions for

internal and external sources that were the basis for many important dosimetry

documents.

4. GEANT (Agostinelliae et al. 2003) - GEometry ANd Tracking, models a variety of different

particles over a range of 250 eV to TeV. Originally developed by CERN for high energy physics.

The latest generation of this software is Geant4,[***] which is widely used in many applications

worldwide.

[***] Copyright (c) Copyright Holders of the Geant4 Collaboration, 1994-2006.

CHAPTER III

METHODS AND MATERIALS

Sample specific activity methods and materials

Samples of bituminous fly ash (N = 30), sub-bituminous fly ash (N = 9), FGD gypsum (N = 20), and scrubber sludges and fixated scrubber sludges (N = 15) from US coals were analyzed using two p-type High Purity Germanium (HPGe) photon detectors, one manufactured by Canberra using the 'Genie 2000'[†††] software and the second by Ortec using the 'GammaVision'[‡‡‡] software. The detectors were calibrated using a mixed nuclide NIST traceable standard used from Eckert & Ziegler and was calibrated in 2008 with a total activity of 7.77×10^4 Bq. The standard contains 100 grams of sand in a 250 mL polypropylene jar. The sample containers were 250 mL (8 oz) polypropylene jars with a cap size of 89 mm from Fisher Scientific. Samples were chosen to be around 40-50 g, so as to be similar to the counting geometry of the standard. The atomic composition of the samples and density of the standard were assumed to be reasonably similar.

Energy calibration of the detector with the standard was necessary before samples could be counted. The procedure for energy calibration for the Ortec is as follows:

[†††] Copyright © 2001 Canberra Industries, Inc.
[‡‡‡] Copyright © 2003 Advanced Measurement Technology, Inc.

1. Place standard in the detector and count for five minutes.

2. Figure 14 shows a spectrum already calibrated with key gammas marked in red, however, in this figure the calibration has already been done, with the ^{137}Cs 661 keV peak showing pertinent information. Before calibration this peak will not display the radionuclide, since there is no information to understand the relationship between channel number and absolute energy.
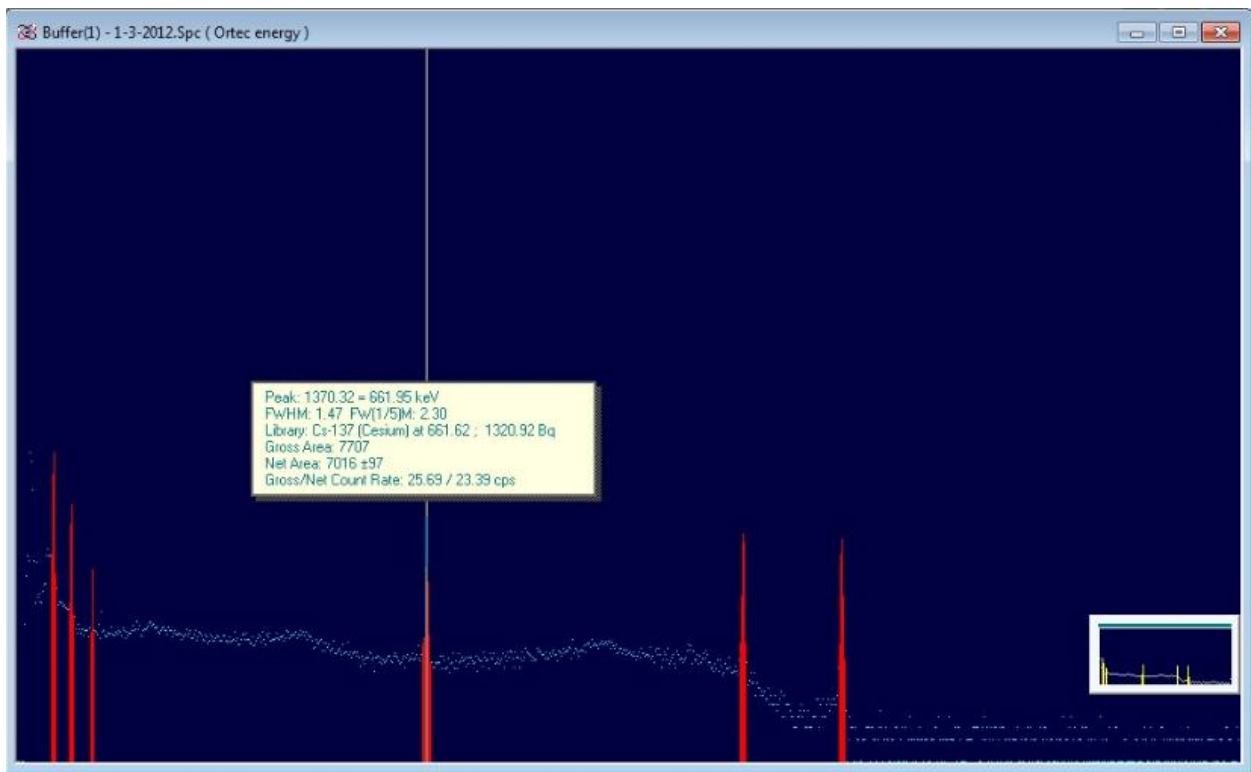
Figure 14. Ortec gamma spectrum.

3. From the spectrum peaks are highlighted and then the radionuclides are identified using the standard calibration sheet, (Appendix A).

4. From the spectrum, the two well-known cobalt peaks at 1173 keV and 1332 keV are easily identified. Other peaks are seen as well; this particular spectrum has

additional peaks at 60, 88, 122 and 662 keV for [241]Am, [109]Cd, [57]57 and [137]Cs

respectively. From these six radionuclides, an energy calibration can be completed.

5. Using the GammaVision software, one can input in these energies for each peak

highlighted as seen below, and a keV vs channel curve for the energy calibration is

created.
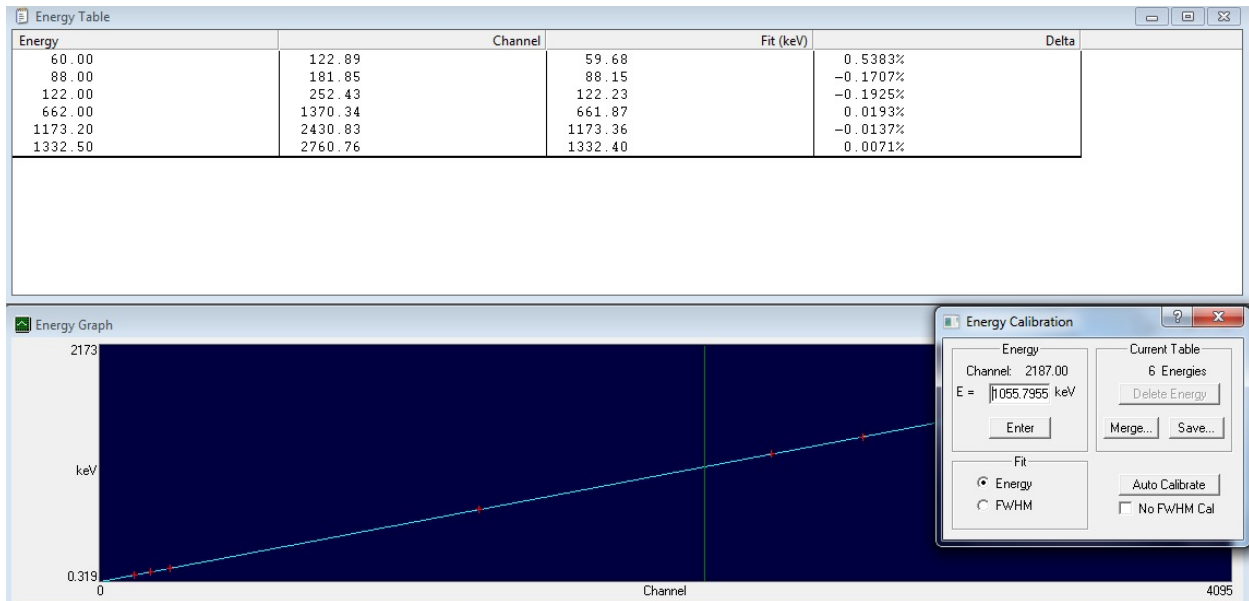
Figure 15. Ortec energy calibration.

The next step before counting samples is to do an efficiency calibration. The procedure

is as follows:

1. Obtain a spectrum from the calibration source for five minutes.

2. Determine the gammas/s for each nuclide after correction for radionuclide decay

since the date of calibration. The original gamma/s is given by the standard

calibration sheet. From the original calibration date, calculate the amount of days

that have passed then use the decay equation to get the correct gamma/s, as shown

below:

$$\left[\frac{gamma}{s}\right]_{present\ day} = \left[\frac{gamma}{s}\right]_{calibration} * e^{-\lambda t}$$

where t = time elapsed in days from calibration

3. Find the counts for each nuclide and divide by the time seconds passed to obtain the

counts per second. The counts per second is divided by the gamma/s,

mathematically shown here:

$$\frac{\left[\frac{counts}{s}\right]}{\left[\frac{gamma}{s}\right]_{present\ day}} = \left[\frac{counts}{gamma}\right]$$

4. The counts/gamma is the efficiency of the detector, efficiency vs energy for the

nuclides, is the efficiency calibration.

5. One can input these numbers into GammaVision and the efficiency calibration is

done, as seen Figure 16.
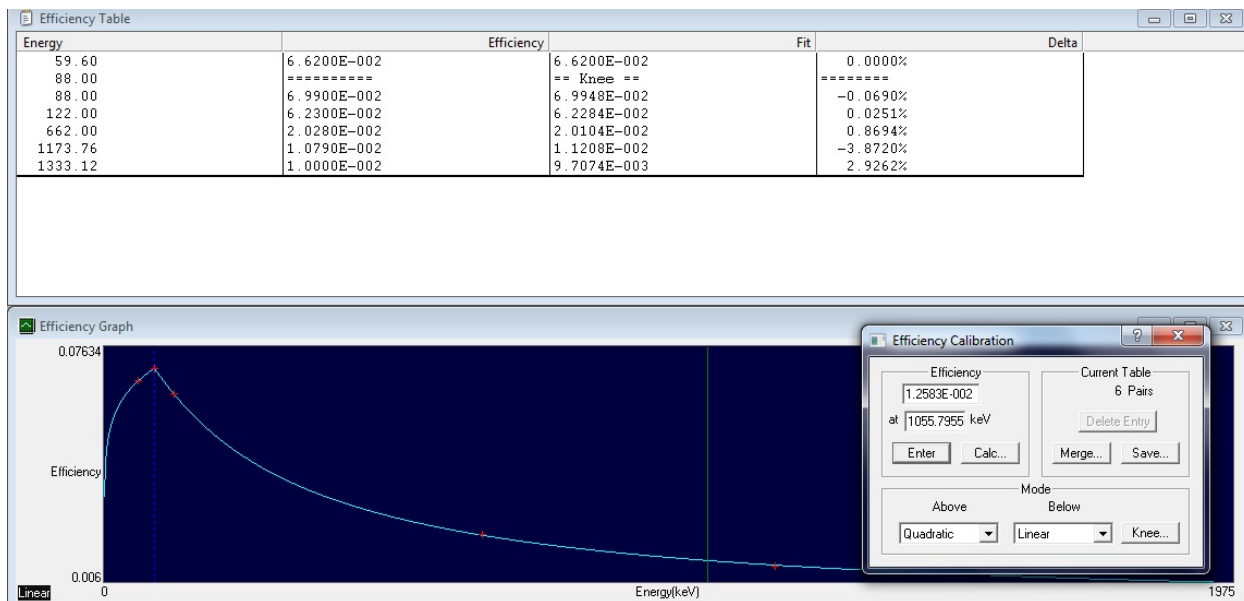
Figure 16. Ortec efficiency calibration curve.

6. The efficiency curve is seen above, with a knee at 88 keV that separates the curve from a quadratic to a linear fit.

The Canberra detector has different software, but the concepts are the same. Once the energy and efficiency calibration were completed counting of fly ash began. Quality Assurance (QA) was performed daily using the standard to confirm that the detector was functioning correctly. The QA method consisted of tracking centroids, full width at half max (FWHM) and net counts of ^{137}Cs and ^{60}Co. Background counts were taken for 12 hours, tracking approximately 10 radionuclides (photopeaks at 186 keV, 352 keV, 511 keV, 661 keV, 1460 keV, and others); a sample container like the ones used to hold the fly ash samples was filled with an amount of deionized water approximately equal to the volume of the samples and placed in the same counting geometry as the samples (the water is to provide some degree of photon scattering similar to what will occur with a sample). Background levels of radon progeny were

variable, so the most recently obtained backgrounds (12 hour) were subtracted before analysis

of the specific activities of the samples. The samples were for sealed for several weeks to allow

for secular equilibrium between the radium parents and the radon progeny. As seen from

Figure 17, it was determined that 4 to 5 half-lives of ^{222}Rn, 3.82 days, would be sufficient to

allow for secular equilibrium. It was assumed that the coal combustion process did not

interfere with isotopic composition, and thus equilibrium between uranium and the other

species down to radon, of the samples; radioactive equilibrium with radon and its progeny was

re-established by sealing the sample containers.
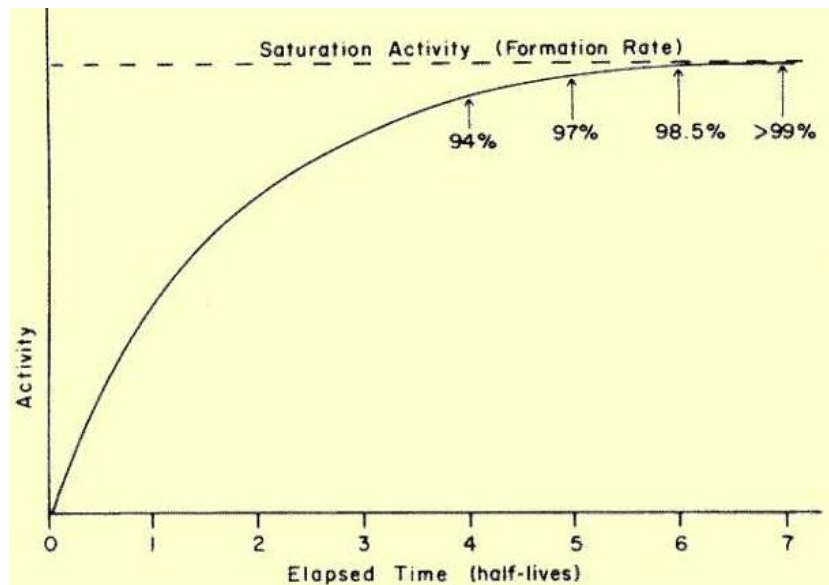
Figure 17. Secular equilibrium plot.

The fly ash samples were counted for eight hours; gypsum samples were counted for 72

hours and scrubber sludge samples for 24 hours; samples were then analyzed using the spectral

analysis software. A number of photopeaks were examined for use in the analysis including:

^{238}U decay series:

> 186 keV (^{226}Ra)
> 295 keV (^{214}Pb)
> 352 keV (^{214}Pb)
> 609 keV (^{214}Bi)
> 1754 keV (^{214}Bi)

^{232}Th decay series:

> 583 keV (^{208}Tl)
> 911 keV (^{228}Ac)

Naturally occurring peaks:

> 511 keV (various)
> 662 keV (^{137}Cs)
> 1460 keV (^{40}K)

For analysis of the uranium and thorium series, one photopeak in each series was used to determine specific activity for all nuclides in the series, rather than an average of multiple photopeaks or other approaches. The 352 keV photopeak of ^{214}Pb, the 583 keV photopeak of ^{208}Tl, and the 1461 keV photopeak of ^{40}K were used to determine the specific activity of ^{238}U, ^{232}Th, and ^{40}K respectively. The partial branching for the ^{208}Tl 583 keV photon was accounted for during analysis. For each sample the MDAs were calculated using the Currie method (Currie 1968). Fly ash samples were separated into bituminous and sub-bituminous categories. Results were graphed using 'box plots' in which the vertical line shows the range, the lower bound of box is the 25th percentile, the middle horizontal line is the median, the upper box is the 75th percentile and outliers are shown as circles. We then compared our results to other data found in the literature. Since most literature studies provide only averages or ranges from a number of samples, box plots could not be performed for these data; instead ranges were given by the

vertical lines with means indicated by circles. Basic plots are given as well, with these plots additional building materials could be placed in the graphs, due to its smaller size. In the bar graphs the whiskers show ± 1 s.d.

Headspace methods and materials

A potential concern arose that, due to the significant amount of headspace in the original containers, radon gas might diffuse out of the sample material and occupy the airspace above the sample. Sample volumes were chosen to be about the same as that of the mixed nuclide calibration sand sample used to determine the detector efficiencies. All of the nuclides in the standard are contained in the (approximately 1 cm) thickness of the material; if radon was partially trapped in the samples, but partially filled the airspace above the samples, the counting geometry difference could result in a difference in the efficiency values. The containers were 89 mm capsize, 8 oz (250 mL) capacity as mentioned earlier. This container left approximately 5 cm of headspace from the 50 grams of fly ash at the bottom to the top of the lid. Figure 18 shows the two containers are the two containers to test this theory, along with the standard.
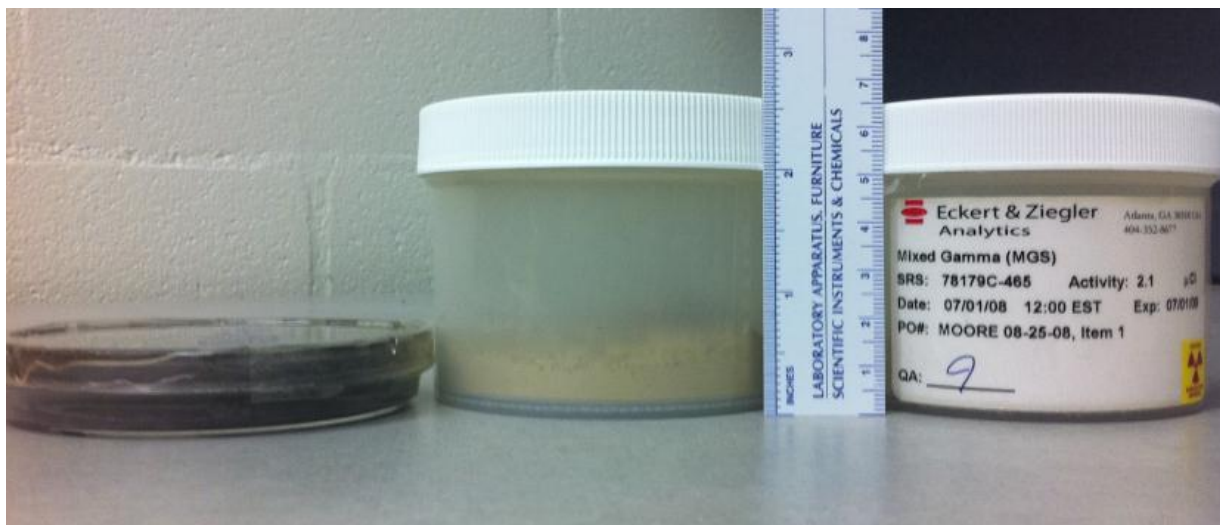
Figure 18. Petri dish, and polypropylene jars for samples and standard and for calibration

Figure 19. Sample containers showing airspace above sample material.

Figure 20. Sample containers showing the diameter of the containers.

The original fly ash concentrations were determined in the larger containers (which are identical to that of the standard). The fly ash samples were taken from the original containers and placed in the smaller petri dishes. The samples were re-weighed and sealed to allow for secular equilibrium. After a month had passed, the samples were recounted. The Canberra detector was used solely for this comparison study, so as to rule out subtle differences between the two detectors. Samples were counted for 8 hours, and background was subtracted (12 hour counts) before results were finalized. The data with and without headspace was compared by calculating the ratio of the two results.

^{222}Rn dose methods and materials

The radon dose from inhalation was estimated using the following equation (Taylor-Lange 2012 et al.)

$$J_f = Q\eta\rho f l_0 \tan h \frac{d}{l_0} \qquad \left[Bq\ m^{-2}\ s^{-1} \right]$$

where J_f = radon exhalation rate from the building element
Q = fly ash mixture specific activity [Bq/kg]
η is the decay constant of radon, $2.1*10^{-6}\ s^{-1}$
ρ is the density of mixture
f is the radon emanating fraction, 5%
l_0 is the diffusion length in concrete, .2 m
d is the half thickness of the building element

$$C_{SS} = \frac{JA}{\lambda V} \qquad \left[Bq\ m^{-3} \right]$$

where C_{ss} = the steady state indoor radon concentration
A = concrete surface area [m^2]
λ = air exchange rate [s^{-1}],
V = volume of the area [m^3]
Assume 25 μSv per Bq m^{-3}

These equations, along with the constants, along with the assumed μSv per Bq m^{-3} conversion factor were taken from Taylor-Lange et al. 2012 and UNSCEAR 1993. For this study, d = 0.125 m, $\lambda = 3.4*10^{-4}s^{-1}$, and A and V were chosen and applied to the different room sizes cited by the EPA as standard room sizes (EPA 2011). The radon dose was taken from room sizes of 6x12x8 ft^3, 10x12x8 ft^3 and 12x15x8 ft^3 for different percentages of fly ash and occupancy factors. The occupancy factors were scaled from an occupancy of 100%, e.g. if the occupancy was 25%, the dose results from 100% were multiplied by 0.25. The percentage of fly ash contributed to a change in both the density of the mixture and the specific activity. The density of concrete was

assumed 2350 kg m^{-3}, while the density of fly ash was assumed to be 1600 kg m^{-3}. If the

mixture was 25%/75% for fly ash and concrete, the density was as follows:

$$\left(2350\ \frac{kg}{m^3} * 0.75\right) + (1600\frac{kg}{m^3} * 0.25) = 2163\frac{kg}{m^3}$$

The specific activity of the sample was found using the same method assuming the specific

activity of concrete being 40, 30 and 400 Bq kg^{-1} as given by the European Commission 112

1999 and fly ash concentrations found in this study using both bituminous and sub-bituminous

results.

Monte Carlo external dose methods

Voxel-based, realistic anthropomorphic phantoms were implemented in the Geant4

Monte Carlo radiation transport simulation environment to estimate yearly doses from usage of

fly ash in concrete. The worst case scenario in terms of dose was estimated to be a concrete

room, e.g. a prison cell, with a person spending approximately 24 hours per day. For other

situations, e.g. homes, offices, occupancy factors will be lower. The simulation was run with 20

million events or disintegrations for ^{238}U and ^{232}Th and 40 million events for ^{40}K. The Monte

Carlo results reported dose in Gy per organ per starting particle, numerically equal to Sv, as

photon radiation weighting factors are 1.0. Effective doses were then calculated using tissue

weighting factors (ICRP 2007).   The yearly dose was found using the following equation:

$$\left[\frac{Sv}{yr}\right] = \frac{V\,[m^3]\rho\left[\frac{kg}{m^3}\right]Q\left[\frac{Bq}{kg}\right]H[Sv] * 3.14 * 10^7[\frac{S}{yr}]}{2 * 10^6 dis}$$

where V = volume of the concrete
ρ = density of the concrete (and fly ash mixture)
Q = specific activity of fly ash
H = total equivalent dose

The same methods were employed for varying room sizes, occupancy factors and fly ash percentages as in the internal radon dose calculations.

An illustration of the Monte Carlo simulation can be seen in Figure 21, with photons both hitting and missing the person represented inside since radiation is random in nature. The walls are made of concrete and the person is standing in the center of the room.
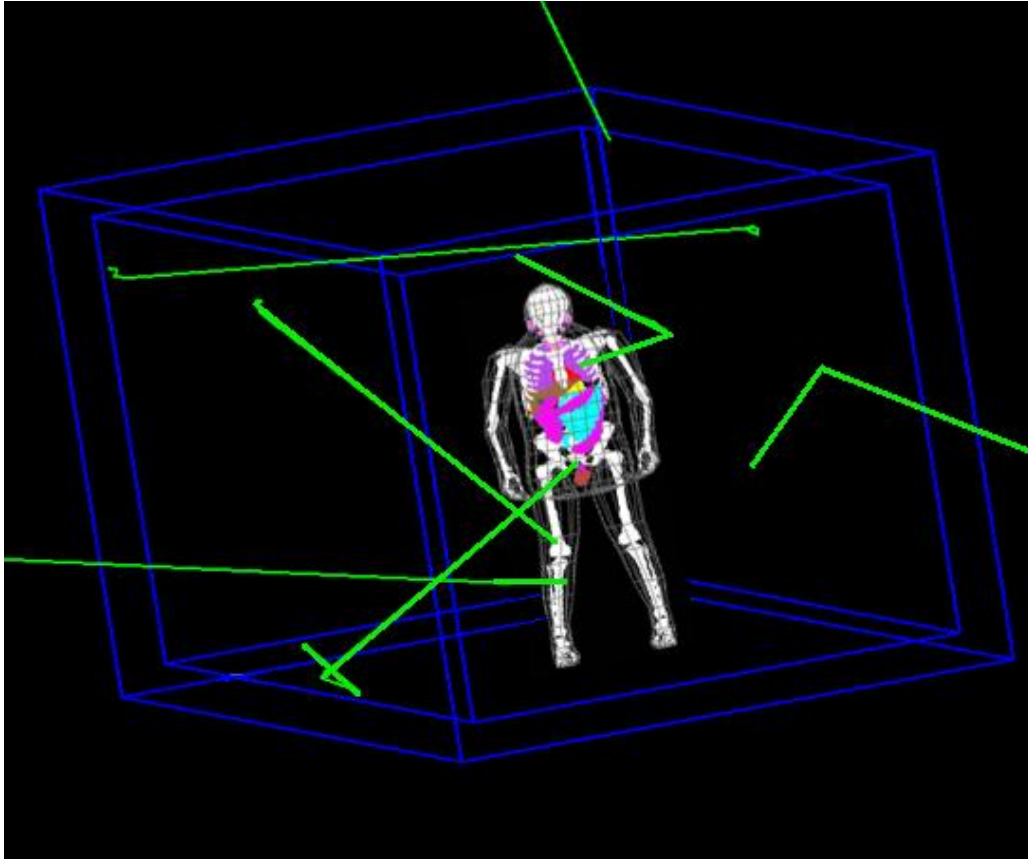
Figure 21. Monte Carlo simulation geometry.

Simulations were performed on a male adult, female adult and male child of ten years. In addition, simulations were done on the male at an offset from half the lateral distance and three-fourths the distance away from the center of the room to determine if position was dependent on the dose received.

CHAPTER IV

RESULTS

Specific activity of fly ash, gypsum and other

All fly ash samples had concentrations of ^{238}U, ^{232}Th, and ^{40}K significantly above system

MDAs. Some gypsum and scrubber sludge sample results for ^{232}Th and ^{40}K were not above

MDA, even with extended sample counting times of up to 72 hours. Tables 11 and 12 show the

results for ^{238}U, ^{232}Th and ^{40}K concentrations in bituminous and sub-bituminous fly ash samples,

with associated statistics (mean, median, standard deviation and range). Table 3 shows the

results of the gypsum samples and Table 4 shows the results for the scrubber sludge samples

and fixated scrubber sludge samples. Figures 22, 23 and 24 give the resulting box plots from

the current study, with comparison to the range of values from the literature cited above for

^{238}U, ^{232}Th and ^{40}K respectively.

Table 11. Bituminous fly ash concentrations (Bq kg^{-1}).

Sample	^{238}U	^{232}Th	^{40}K
1	125	90	606
2	124	86	617
3	217	97	790
4	152	101	462
5	68	58	630
6	181	120	576
7	135	103	547
8	131	91	552
9	130	99	758
10	51	39	426
11	147	77	641
12	103	78	534
13	136	90	738
14	166	108	694
15	138	84	773
16	106	89	693
17	132	85	552
18	97	73	432
19	110	82	741
20	209	71	735
21	119	63	216
22	79	35	177
23	117	66	518
24	90	10	750
25	47	37	287
26	30	35	369
27	54	33	244
28	92	69	506
29	180	60	928
30	108	78	574
Mean	119	73	569
Standard Deviation	45	26	184
Min	30	10	177
Max	217	120	928
Median	119	77	571

Table 12. Sub-bituminous fly ash concentrations (Bq kg^{-1}).

Sample name	^{238}U	^{232}Th	^{40}K
1	98	71	303
2	209	110	245
3	119	93	115
4	127	91	158
5	81	60	87
6	120	94	195
7	72	53	162
8	94	76	108
9	111	84	168
Mean	115	81	171
Standard Deviation	40	18	69
Min	72	53	87
Max	209	110	303
Median	111	84	162

Table 13. Gypsum concentrations (Bq kg^{-1}).

Sample name	^{238}U	^{232}Th	^{40}K
1	4	1	8
2	5	---	10
3	7	1	8
4	1	---	13
5	11	1	2
6	10	1	0.5
7	7	1	7
8	9	0.3	11
9	3	---	16
10	24	3	---
11	6	1	12
12	12	2	17
13	12	2	16
14	8	0.2	11
15	10	---	---
16	8	1	19
17	14	---	4
18	14	---	---
19	11	1	5
20	11	1	---
Mean	9	1	10
Standard Deviation	5	1	5
Min	1	---	---
Max	24	3	19
Median	10	1	11

Table 14. Scrubber sludges and fixated scrubber sludges concentrations (Bq kg^{-1}).

Sample name	^{238}U	^{232}Th	^{40}K
1	117	69	455
2	6	---	53
3	10	---	24
4	16	6	123
5	114	85	541
6	12	---	13
7	40	17	335
8	19	13	148
9	7	---	9
10	0.2	0.3	9
11	23	16	167
12	109	9	239
13	95	10	94
14	135	3	69
15	174	10	177
Mean	58	22	164
Standard Deviation	58	28	165
Min	0.2	---	9
Max	174	85	541
Median	23	10	123
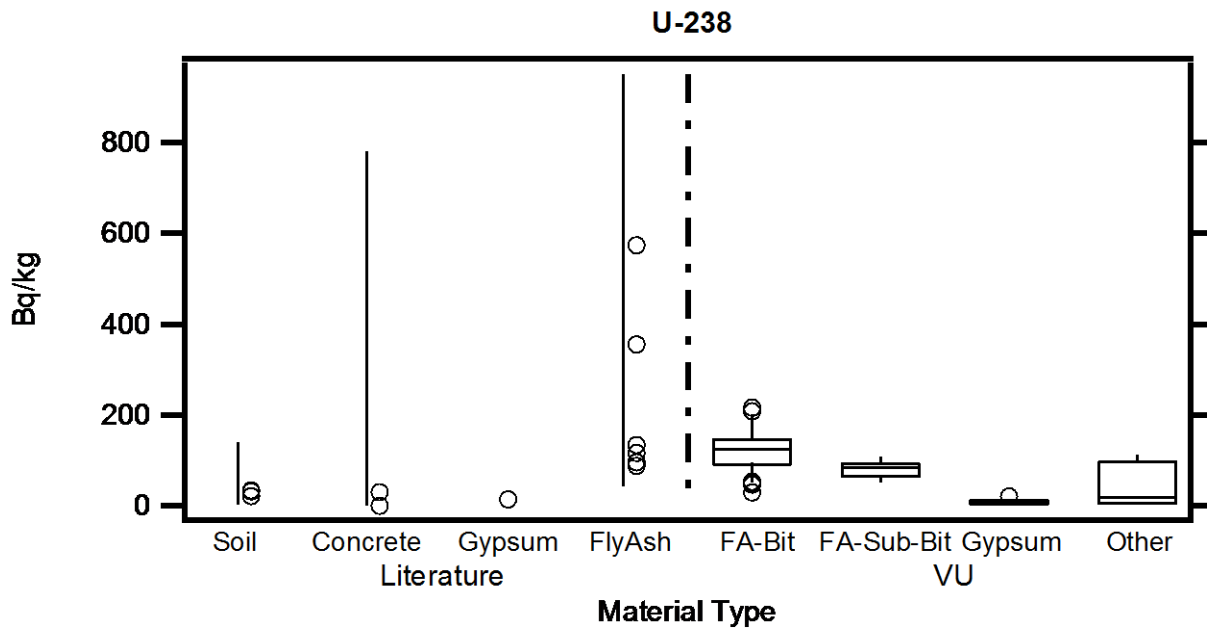
Figure 22. ^{238}U results from this study, compared to values observed in the literature.
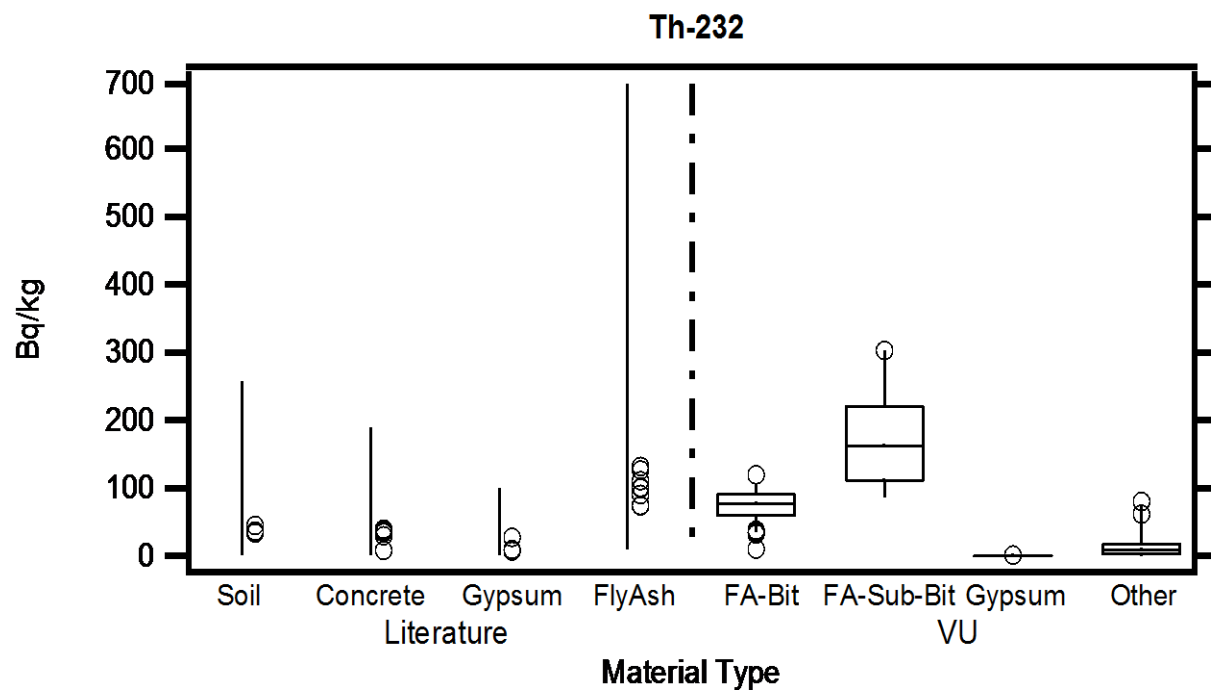
Figure 23. [232]Th results from this study, compared to values observed in the literature.
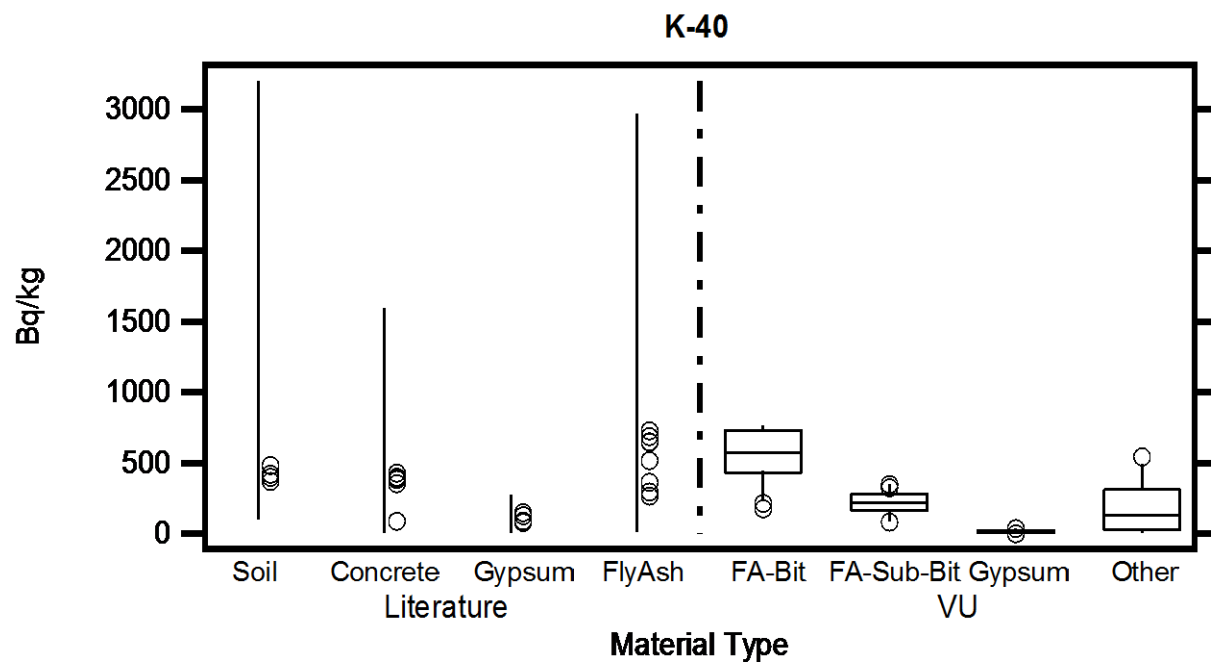
Figure 24. ^{40}K results from this study, compared to values observed in the literature.
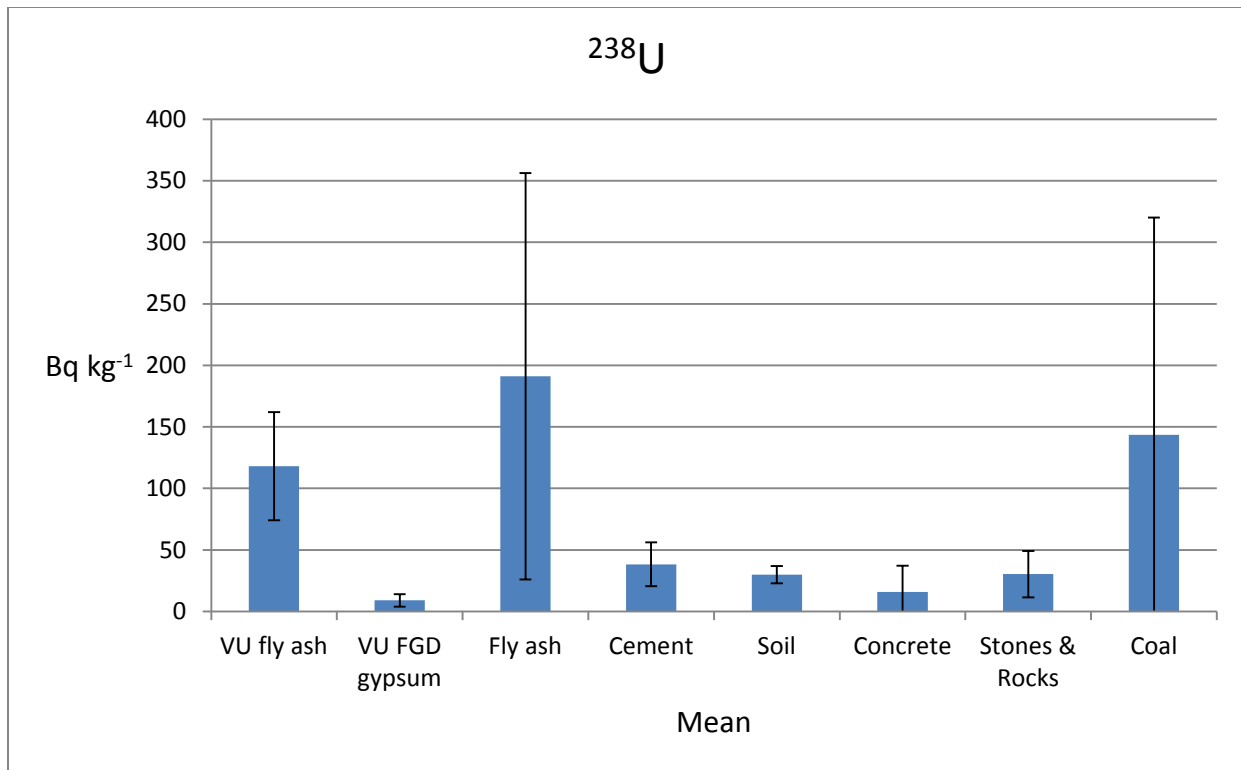
Figure 25. ^{238}U concentrations; error bars are ± 1 standard deviation.
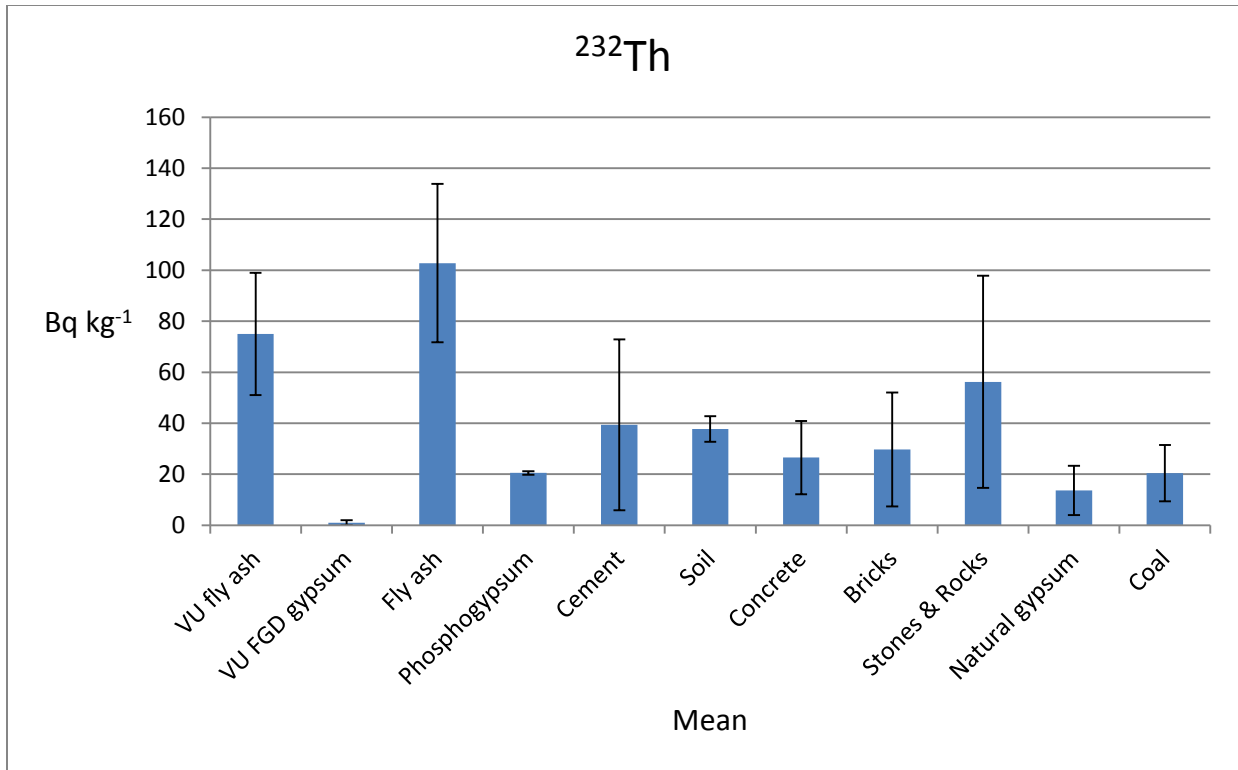
Figure 26. ^{232}Th concentrations; error bars are ± 1 standard deviation.
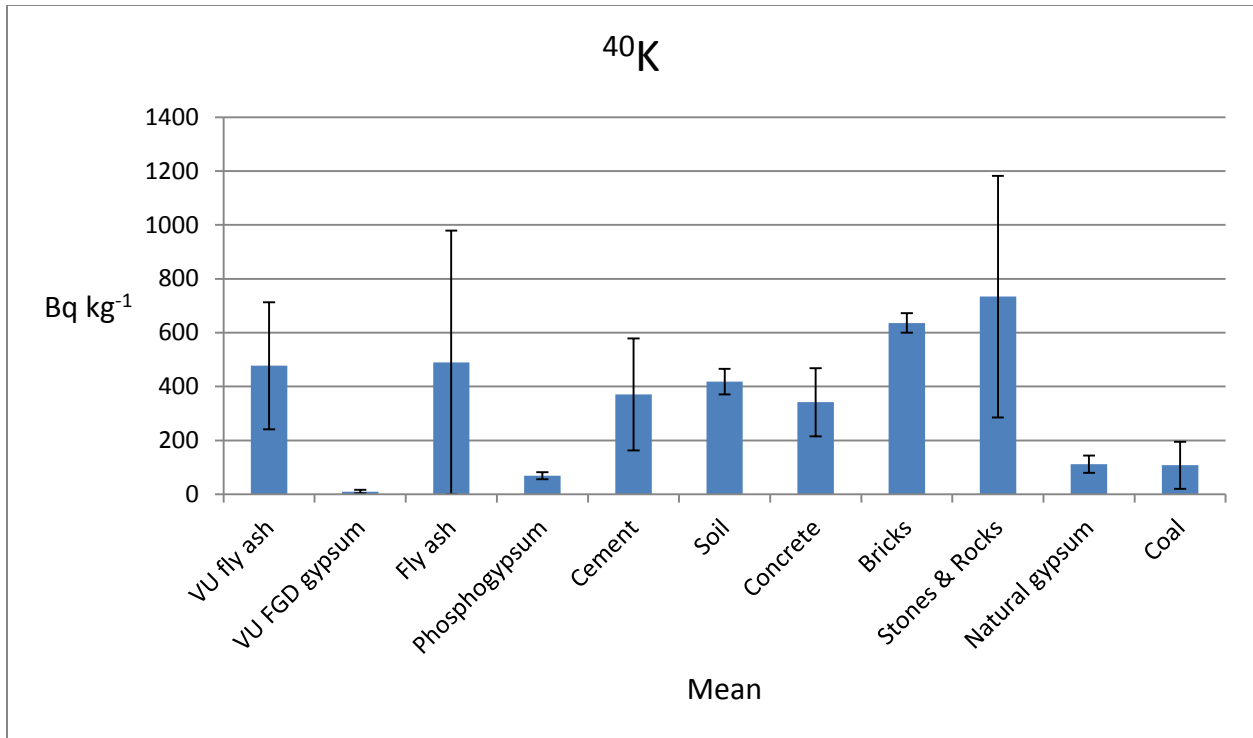
Figure 27. ^{40}K concentrations; error bars are ± 1 standard deviation.

Headspace comparison

Table 15. ^{238}U concentrations in the larger containers (headspace) and Petri dishes (no headspace).

Sample name	Headspace ^{238}U (Bq kg^{-1})	No head space ^{238}U (Bq kg^{-1})	Ratio
1	125	137	1.10
2	123	155	1.25
3	217	250	1.15
4	152	222	1.45
5	68	80	1.18
6	181	219	1.21
7	135	142	1.05
8	131	193	1.48
9	130	150	1.15
10	51	89	1.77
11	147	178	1.21
12	103	131	1.27
13	136	160	1.17
14	166	194	1.16
15	138	165	1.19
16	106	122	1.14
17	132	150	1.14
18	97	113	1.16
19	110	118	1.07
20	209	241	1.15
21	119	149	1.25
22	79	128	1.61
23	117	134	1.14
24	90	124	1.38
25	47	111	2.34
26	30	83	2.71
27	54	73	1.35
28	92	101	1.10
29	180	203	1.12
30	108	126	1.17
31	98	123	1.25
32	209	239	1.14
33	119	130	1.09
34	127	144	1.13
35	81	82	1.02

Table 15, continued

36	120	141	1.18
37	72	79	1.10
38	94	108	1.16
39	111	123	1.11
Average	118	144	1.28
Standard Deviation	44	47	
Variance	1914	2216	

Table 16. ^{232}Th concentrations in the larger containers (headspace) and Petri dishes (no headspace).

Sample name	Headspace ^{232}Th (Bq kg^{-1})	No head space ^{232}Th (Bq kg^{-1})	Ratio
1	90	90	1.00
2	85	91	1.07
3	97	119	1.23
4	101	115	1.14
5	58	60	1.02
6	120	118	0.99
7	103	114	1.11
8	91	131	1.44
9	99	106	1.07
10	39	59	1.54
11	77	104	1.34
12	78	96	1.24
13	90	106	1.19
14	108	122	1.13
15	84	112	1.34
16	89	93	1.05
17	85	92	1.08
18	73	77	1.06
19	82	97	1.18
20	71	79	1.11
21	63	74	1.18
22	35	54	1.56
23	66	73	1.11
24	10	91	8.77
25	37	107	2.93
26	35	40	1.15

Table 16, continued

27	33	37	1.11
28	69	68	0.98
29	60	60	1.01
30	78	94	1.21
31	71	85	1.20
32	110	114	1.04
33	93	101	1.08
34	91	93	1.03
35	60	58	0.97
36	94	102	1.09
37	53	56	1.06
38	76	84	1.10
39	84	91	1.08
Average	75	89	1.38
Standard Deviation	24	23	1.25
Variance	594	549	

Table 17. ^{40}K concentrations in the larger containers (headspace) and Petri dishes (no headspace).

Sample name	Headspace ^{40}K (Bq kg^{-1})	No head space ^{40}K (Bq kg^{-1})	Ratio
1	606	687	1.13
2	616	686	1.11
3	790	814	1.03
4	462	786	1.70
5	630	776	1.23
6	576	758	1.31
7	547	541	0.99
8	552	857	1.55
9	758	899	1.19
10	426	767	1.80
11	641	772	1.21
12	534	682	1.28
13	738	861	1.17
14	694	784	1.13
15	773	928	1.20
16	693	928	1.34

Table 17, continued

17	552	730	1.32
18	432	574	1.33
19	741	891	1.20
20	735	896	1.22
21	216	320	1.48
22	177	303	1.71
23	518	621	1.20
24	750	890	1.19
25	287	813	2.83
26	369	442	1.20
27	244	334	1.37
28	506	630	1.24
29	928	1083	1.17
30	574	783	1.37
31	303	361	1.19
32	245	314	1.28
33	115	175	1.52
34	158	133	0.84
35	87	80	0.92
36	195	225	1.15
37	162	144	0.88
38	108	183	1.69
39	168	167	0.99
Average	477	606	1.27
Standard Deviation	236	284	1.20
Variance	56	81	

Internal dose due to ^{222}Rn

Table 18. Doses from ^{222}Rn inhalation (mSv y^{-1}), occupancy of 100%, concrete concentration 40 Bq kg^{-1}.

Type; FA%/Concrete%	Room size	Indoor radon concentration Bq m^{-3}	mSv y^{-1}
	6x12x8 ft^3	10.29	0.26
	10x12x8 ft^3	8.46	0.21
Bituminous FA; 25/75	15x12x8 ft^3	7.54	0.19
	6x12x8 ft^3	10.11	0.25
	10x12x8 ft^3	8.32	0.21
Sub-bituminous; 25/75	15x12x8 ft^3	7.42	0.19
	6x12x8 ft^3	7.48	0.19
	10x12x8 ft^3	6.15	0.15
Concrete; 0/100	15x12x8 ft^3	5.49	0.14
	6x12x8 ft^3	9.24	0.23
	10x12x8 ft^3	7.59	0.19
Bituminous FA; 15/85	15x12x8 ft^3	6.77	0.17
	6x12x8 ft^3	9.13	0.23
	10x12x8 ft^3	7.51	0.19
Sub-bituminous FA; 15/85	15x12x8 ft^3	6.69	0.17
	6x12x8 ft^3	8.09	0.20
	10x12x8 ft^3	6.65	0.17
Bituminous FA; 5/95	15x12x8 ft^3	5.93	0.15
	6x12x8 ft^3	8.05	0.20
	10x12x8 ft^3	6.62	0.17
Sub-bituminous FA; 5/95	15x12x8 ft^3	5.91	0.15

Table 19. Doses from Indoor ^{222}Rn inhalation (mSv y^{-1}) occupancy of 65% and 25%; concrete concentration assuming 40 Bq kg^{-1}.

Type	Room size	occ .65, mSv yr^{-1}	occ .25, mSv yr^{-1}
Bituminous	6x12x8 ft^3	0.17	0.064
	10x12x8 ft^3	0.14	0.053
	12x15x8 ft^3	0.12	0.047
Sub-bituminous	6x12x8 ft^3	0.16	0.063
	10x12x8 ft^3	0.14	0.052
	12x15x8 ft^3	0.12	0.046
Concrete, no FA	6x12x8 ft^3	0.12	0.047
	10x12x8 ft^3	0.10	0.038
	12x15x8 ft^3	0.090	0.034
Bituminous; 15%, 85%	6x12x8 ft^3	0.15	0.058
	10x12x8 ft^3	0.12	0.047
	12x15x8 ft^3	0.11	0.042
Sub-bituminous; 15%, 85%	6x12x8 ft^3	0.15	0.057
	10x12x8 ft^3	0.12	0.047
	12x15x8 ft^3	0.11	0.042
Bituminous; 5%, 95%	6x12x8 ft^3	0.13	0.051
	10x12x8 ft^3	0.11	0.042
	12x15x8 ft^3	0.10	0.037
Sub-bituminous; 5%, 95%	6x12x8 ft^3	0.13	0.050
	10x12x8 ft^3	0.11	0.041
	12x15x8 ft^3	0.10	0.037

External dose from Monte Carlo simulations

Table 20. External dose (mSv y^{-1}), occupancy of 100%, adult male.

Type; FA%/Concrete%	Room size	^{238}U	^{232}Th	^{40}K	Total
Bituminous FA; 25/75	6x12x8 ft^3	0.51	0.24	0.17	0.92
	10x12x8 ft^3	0.53	0.26	0.17	0.96
	12x15x8 ft^3	0.50	0.25	0.18	0.94
Sub-bituminous; 25/75	6x12x8 ft^3	0.50	0.26	0.13	0.89
	10x12x8 ft^3	0.52	0.27	0.14	0.93
	12x15x8 ft^3	0.49	0.26	0.14	0.90
Concrete; 0/100	6x12x8 ft^3	0.36	0.19	0.16	0.70
	10x12x8 ft^3	0.37	0.20	0.16	0.73
	12x15x8 ft^3	0.35	0.19	0.17	0.71
Bituminous FA; 15/85	6x12x8 ft^3	0.45	0.22	0.17	0.84
	10x12x8 ft^3	0.47	0.23	0.17	0.88
	12x15x8 ft^3	0.44	0.23	0.18	0.86
Sub-bituminous FA; 15/85	6x12x8 ft^3	0.45	0.23	0.14	0.82
	10x12x8 ft^3	0.47	0.24	0.15	0.86
	12x15x8 ft^3	0.44	0.24	0.16	0.83
Bituminous FA; 5/95	6x12x8 ft^3	0.39	0.20	0.16	0.75
	10x12x8 ft^3	0.41	0.21	0.16	0.78
	12x15x8 ft^3	0.38	0.21	0.17	0.76
Sub-bituminous FA; 5/95	6x12x8 ft^3	0.39	0.20	0.15	0.74
	10x12x8 ft^3	0.40	0.21	0.16	0.77
	12x15x8 ft^3	0.38	0.21	0.17	0.76

Table 21. External dose (mSv y^{-1}), occupancy of 65%, adult male.

Type; FA%/Concrete%	Room size	^{238}U	^{232}Th	^{40}K	Total
Bituminous FA; 25/75	6x12x8 ft^3	0.33	0.16	0.11	0.60
	10x12x8 ft^3	0.35	0.17	0.11	0.62
	12x15x8 ft^3	0.33	0.16	0.12	0.61
Sub-bituminous; 25/75	6x12x8 ft^3	0.33	0.166	0.09	0.58
	10x12x8 ft^3	0.34	0.175	0.09	0.60
	12x15x8 ft^3	0.32	0.172	0.09	0.59
Concrete; 0/100	6x12x8 ft^3	0.23	0.12	0.10	0.45
	10x12x8 ft^3	0.24	0.13	0.10	0.47
	12x15x8 ft^3	0.23	0.13	0.11	0.46
Bituminous FA; 15/85	6x12x8 ft^3	0.30	0.15	0.11	0.55
	10x12x8 ft^3	0.31	0.15	0.11	0.57
	12x15x8 ft^3	0.29	0.15	0.12	0.56
Sub-bituminous FA; 15/85	6x12x8 ft^3	0.29	0.150	0.09	0.53
	10x12x8 ft^3	0.30	0.16	0.10	0.56
	12x15x8 ft^3	0.29	0.15	0.10	0.54
Bituminous FA; 5/95	6x12x8 ft^3	0.25	0.13	0.10	0.49
	10x12x8 ft^3	0.26	0.14	0.11	0.51
	12x15x8 ft^3	0.25	0.13	0.11	0.50
Sub-bituminous FA; 5/95	6x12x8 ft^3	0.25	0.13	0.10	0.48
	10x12x8 ft^3	0.26	0.14	0.10	0.50
	12x15x8 ft^3	0.25	0.14	0.11	0.49

Table 22. External dose (mSv y^{-1}), occupancy of 25%, adult male.

Type; FA%/Concrete%	Room size	U-238	Th-232	K-40	Total
Bituminous FA; 25/75	6x12x8 ft^3	0.13	0.061	0.042	0.23
	10x12x8 ft^3	0.133	0.064	0.043	0.24
	12x15x8 ft^3	0.125	0.063	0.046	0.23
Sub-bituminous; 25/75	6x12x8 ft^3	0.13	0.064	0.033	0.22
	10x12x8 ft^3	0.131	0.067	0.034	0.23
	12x15x8 ft^3	0.123	0.066	0.036	0.23
Concrete; 0/100	6x12x8 ft^3	0.089	0.047	0.039	0.17
	10x12x8 ft^3	0.093	0.049	0.040	0.18
	12x15x8 ft^3	0.087	0.048	0.043	0.18
Bituminous FA; 15/85	6x12x8 ft^3	0.11	0.056	0.041	0.21
	10x12x8 ft^3	0.118	0.059	0.042	0.22
	12x15x8 ft^3	0.111	0.058	0.045	0.21
Sub-bituminous FA; 15/85	6x12x8 ft^3	0.11	0.058	0.036	0.21
	10x12x8 ft^3	0.117	0.061	0.037	0.21
	12x15x8 ft^3	0.110	0.060	0.039	0.21
Bituminous FA; 5/95	6x12x8 ft^3	0.10	0.050	0.040	0.19
	10x12x8 ft^3	0.101	0.052	0.041	0.19
	12x15x8 ft^3	0.096	0.052	0.043	0.19
Sub-bituminous FA; 5/95	6x12x8 ft^3	0.10	0.050	0.038	0.19
	10x12x8 ft^3	0.101	0.053	0.039	0.19
	12x15x8 ft^3	0.095	0.052	0.041	0.19

Table 23. External dose (mSv y^{-1}), occupancy of 100%, adult female.

Type; FA%/Concrete%	Room size	^{238}U	^{232}Th	^{40}K	Total
Bituminous FA; 25/75	6x12x8 ft^3	0.60	0.30	0.20	1.10
	10x12x8 ft^3	0.61	0.30	0.21	1.12
	12x15x8 ft^3	0.59	0.30	0.21	1.10
Sub-bituminous; 25/75	6x12x8 ft^3	0.59	0.31	0.16	1.06
	10x12x8 ft^3	0.60	0.32	0.16	1.08
	12x15x8 ft^3	0.58	0.31	0.17	1.06
Concrete; 0/100	6x12x8 ft^3	0.42	0.23	0.19	0.83
	10x12x8 ft^3	0.42	0.23	0.19	0.85
	12x15x8 ft^3	0.41	0.23	0.20	0.83
Bituminous FA; 15/85	6x12x8 ft^3	0.53	0.27	0.20	1.01
	10x12x8 ft^3	0.54	0.28	0.20	1.02
	12x15x8 ft^3	0.52	0.27	0.21	1.00
Sub-bituminous FA; 15/85	6x12x8 ft^3	0.53	0.28	0.17	0.98
	10x12x8 ft^3	0.53	0.29	0.17	0.99
	12x15x8 ft^3	0.52	0.28	0.18	0.98
Bituminous FA; 5/95	6x12x8 ft^3	0.46	0.25	0.19	0.90
	10x12x8 ft^3	0.46	0.25	0.19	0.91
	12x15x8 ft^3	0.45	0.24	0.20	0.89
Sub-bituminous FA; 5/95	6x12x8 ft^3	0.46	0.25	0.18	0.89
	10x12x8 ft^3	0.46	0.25	0.19	0.90
	12x15x8 ft^3	0.45	0.25	0.19	0.88

Table 24. External dose (mSv y^{-1}), occupancy of 65%, adult female.

Type; FA%/Concrete%	Room size	^{238}U	^{232}Th	^{40}K	Total
Bituminous FA; 25/75	6x12x8 ft^3	0.39	0.20	0.13	0.72
	10x12x8 ft^3	0.39	0.20	0.13	0.72
	12x15x8 ft^3	0.38	0.19	0.14	0.71
Sub-bituminous; 25/75	6x12x8 ft^3	0.38	0.20	0.10	0.69
	10x12x8 ft^3	0.39	0.21	0.11	0.70
	12x15x8 ft^3	0.38	0.20	0.11	0.69
Concrete; 0/100	6x12x8 ft^3	0.27	0.15	0.12	0.54
	10x12x8 ft^3	0.27	0.15	0.12	0.55
	12x15x8 ft^3	0.27	0.15	0.13	0.54
Bituminous FA; 15/85	6x12x8 ft^3	0.35	0.18	0.13	0.65
	10x12x8 ft^3	0.35	0.18	0.13	0.66
	12x15x8 ft^3	0.34	0.18	0.13	0.65
Sub-bituminous FA; 15/85	6x12x8 ft^3	0.34	0.18	0.11	0.64
	10x12x8 ft^3	0.35	0.19	0.11	0.65
	12x15x8 ft^3	0.34	0.18	0.12	0.64
Bituminous FA; 5/95	6x12x8 ft^3	0.30	0.16	0.12	0.58
	10x12x8 ft^3	0.30	0.16	0.13	0.59
	12x15x8 ft^3	0.29	0.16	0.13	0.58
Sub-bituminous FA; 5/95	6x12x8 ft^3	0.30	0.16	0.12	0.58
	10x12x8 ft^3	0.30	0.16	0.12	0.58
	12x15x8 ft^3	0.29	0.16	0.12	0.58

Table 25. External dose (mSv y^{-1}), occupancy of 25%, adult female.

Type; FA%/Concrete%	Room size	^{238}U	^{232}Th	^{40}K	Total
Bituminous FA; 25/75	6x12x8 ft^3	0.15	0.075	0.050	0.28
	10x12x8 ft^3	0.15	0.076	0.051	0.28
	12x15x8 ft^3	0.15	0.074	0.053	0.27
Sub-bituminous; 25/75	6x12x8 ft^3	0.15	0.079	0.039	0.27
	10x12x8 ft^3	0.15	0.080	0.040	0.27
	12x15x8 ft^3	0.14	0.078	0.042	0.26
Concrete; 0/100	6x12x8 ft^3	0.10	0.057	0.046	0.21
	10x12x8 ft^3	0.11	0.058	0.048	0.21
	12x15x8 ft^3	0.10	0.057	0.049	0.21
Bituminous FA; 15/85	6x12x8 ft^3	0.13	0.069	0.049	0.25
	10x12x8 ft^3	0.13	0.070	0.050	0.25
	12x15x8 ft^3	0.13	0.068	0.052	0.25
Sub-bituminous FA; 15/85	6x12x8 ft^3	0.13	0.071	0.042	0.25
	10x12x8 ft^3	0.13	0.072	0.043	0.25
	12x15x8 ft^3	0.13	0.070	0.045	0.24
Bituminous FA; 5/95	6x12x8 ft^3	0.11	0.061	0.047	0.22
	10x12x8 ft^3	0.12	0.062	0.049	0.23
	12x15x8 ft^3	0.11	0.061	0.050	0.22
Sub-bituminous FA; 5/95	6x12x8 ft^3	0.11	0.062	0.045	0.22
	10x12x8 ft^3	0.12	0.063	0.046	0.22
	12x15x8 ft^3	0.11	0.061	0.048	0.22

Table 26. External dose (mSv y^{-1}), occupancy of 100%, 10 year old male.

Type; FA%/Concrete%	Room size	^{238}U	^{232}Th	^{40}K	Total
Bituminous FA; 25/75	6x12x8 ft^3	0.57	0.29	0.20	1.05
	10x12x8 ft^3	0.61	0.28	0.19	1.08
	12x15x8 ft^3	0.55	0.29	0.23	1.06
Sub-bituminous; 25/75	6x12x8 ft^3	0.56	0.30	0.16	1.02
	10x12x8 ft^3	0.60	0.30	0.15	1.05
	12x15x8 ft^3	0.54	0.30	0.18	1.02
Concrete; 0/100	6x12x8 ft^3	0.40	0.22	0.18	0.80
	10x12x8 ft^3	0.43	0.22	0.17	0.82
	12x15x8 ft^3	0.38	0.22	0.21	0.81
Bituminous FA; 15/85	6x12x8 ft^3	0.48	0.25	0.18	0.91
	10x12x8 ft^3	0.54	0.26	0.18	0.99
	12x15x8 ft^3	0.49	0.27	0.22	0.97
Sub-bituminous FA; 15/85	6x12x8 ft^3	0.50	0.27	0.17	0.94
	10x12x8 ft^3	0.51	0.25	0.15	0.91
	12x15x8 ft^3	0.48	0.27	0.19	0.95
Bituminous FA; 5/95	6x12x8 ft^3	0.43	0.23	0.19	0.86
	10x12x8 ft^3	0.47	0.23	0.18	0.88
	12x15x8 ft^3	0.42	0.24	0.21	0.87
Sub-bituminous FA; 5/95	6x12x8 ft^3	0.43	0.24	0.18	0.85
	10x12x8 ft^3	0.47	0.23	0.17	0.87
	12x15x8 ft^3	0.42	0.24	0.20	0.86

Table 27. External dose (mSv y^{-1}), occupancy of 65%, 10 year old male.

Type; FA%/Concrete%	Room size	^{238}U	^{232}Th	^{40}K	Total
Bituminous FA; 25/75	6x12x8 ft^3	0.37	0.19	0.13	0.68
	10x12x8 ft^3	0.40	0.18	0.12	0.70
	12x15x8 ft^3	0.36	0.19	0.15	0.69
Sub-bituminous; 25/75	6x12x8 ft^3	0.36	0.196	0.10	0.66
	10x12x8 ft^3	0.39	0.192	0.10	0.68
	12x15x8 ft^3	0.35	0.198	0.12	0.66
Concrete; 0/100	6x12x8 ft^3	0.26	0.14	0.12	0.52
	10x12x8 ft^3	0.28	0.14	0.11	0.53
	12x15x8 ft^3	0.25	0.14	0.14	0.53
Bituminous FA; 15/85	6x12x8 ft^3	0.31	0.16	0.12	0.59
	10x12x8 ft^3	0.35	0.17	0.12	0.64
	12x15x8 ft^3	0.32	0.17	0.14	0.63
Sub-bituminous FA; 15/85	6x12x8 ft^3	0.32	0.176	0.11	0.61
	10x12x8 ft^3	0.33	0.16	0.10	0.59
	12x15x8 ft^3	0.31	0.18	0.12	0.61
Bituminous FA; 5/95	6x12x8 ft^3	0.28	0.15	0.12	0.56
	10x12x8 ft^3	0.30	0.15	0.12	0.57
	12x15x8 ft^3	0.27	0.15	0.14	0.56
Sub-bituminous FA; 5/95	6x12x8 ft^3	0.28	0.15	0.12	0.55
	10x12x8 ft^3	0.30	0.15	0.11	0.57
	12x15x8 ft^3	0.27	0.16	0.13	0.56

Table 28. External dose (mSv y^{-1}), occupancy of 25%, 10 year old male.

Type; FA%/Concrete%	Room size	^{238}U	^{232}Th	^{40}K	Total
Bituminous FA; 25/75	6x12x8 ft^3	0.14	0.072	0.050	0.26
	10x12x8 ft^3	0.15	0.071	0.047	0.27
	12x15x8 ft^3	0.14	0.073	0.056	0.27
Sub-bituminous; 25/75	6x12x8 ft^3	0.14	0.075	0.039	0.25
	10x12x8 ft^3	0.15	0.074	0.037	0.26
	12x15x8 ft^3	0.13	0.076	0.044	0.25
Concrete; 0/100	6x12x8 ft^3	0.10	0.055	0.046	0.20
	10x12x8 ft^3	0.11	0.054	0.044	0.20
	12x15x8 ft^3	0.10	0.055	0.052	0.20
Bituminous FA; 15/85	6x12x8 ft^3	0.12	0.062	0.046	0.23
	10x12x8 ft^3	0.14	0.065	0.046	0.25
	12x15x8 ft^3	0.12	0.066	0.055	0.24
Sub-bituminous FA; 15/85	6x12x8 ft^3	0.12	0.068	0.042	0.23
	10x12x8 ft^3	0.13	0.063	0.038	0.23
	12x15x8 ft^3	0.12	0.069	0.048	0.24
Bituminous FA; 5/95	6x12x8 ft^3	0.11	0.059	0.047	0.21
	10x12x8 ft^3	0.12	0.058	0.045	0.22
	12x15x8 ft^3	0.10	0.059	0.053	0.22
Sub-bituminous FA; 5/95	6x12x8 ft^3	0.11	0.059	0.045	0.21
	10x12x8 ft^3	0.12	0.058	0.042	0.22
	12x15x8 ft^3	0.10	0.060	0.051	0.21

Table 29. External dose halfway across room (mSv y^{-1}), occupancy of 100%, adult male, 10x12x8 ft^3.

Type; FA%/Concrete%	^{238}U	^{232}Th	^{40}K	Total
Bituminous FA; 25/75	0.52	0.25	0.18	0.95
Sub-bituminous FA; 25/75	0.51	0.27	0.14	0.92
Concrete; 0/100	0.36	0.19	0.17	0.72
Bituminous FA; 15/85	0.46	0.23	0.17	0.87
Sub-bituminous FA; 15/85	0.46	0.24	0.15	0.85
Bituminous FA; 5/95	0.40	0.21	0.17	0.77
Sub-bituminous FA; 5/95	0.40	0.21	0.16	0.77

Table 30. External dose halfway across room (mSv y^{-1}), occupancy of 65%, adult male, 10x12x8 ft^3.

Type; FA%/Concrete%	U-238	Th-232	K-40	Total
Bituminous FA; 25/75	0.34	0.16	0.12	0.62
Sub-bituminous FA; 25/75	0.33	0.17	0.09	0.60
Concrete; 0/100	0.24	0.13	0.11	0.47
Bituminous FA; 15/85	0.30	0.15	0.11	0.57
Sub-bituminous FA; 15/85	0.30	0.16	0.10	0.55
Bituminous FA; 5/95	0.26	0.13	0.11	0.50
Sub-bituminous FA; 5/95	0.26	0.14	0.10	0.50

Table 31. External dose halfway across room (mSv y^{-1}), occupancy of 25%, adult male, 10x12x8 ft^3.

Type; FA%/Concrete%	^{238}U	^{232}Th	^{40}K	Total
Bituminous FA; 25/75	0.13	0.063	0.044	0.24
Sub-bituminous FA; 25/75	0.13	0.066	0.035	0.23
Concrete; 0/100	0.09	0.048	0.041	0.18
Bituminous FA; 15/85	0.12	0.058	0.044	0.22
Sub-bituminous FA; 15/85	0.11	0.060	0.038	0.21
Bituminous FA; 5/95	0.10	0.052	0.042	0.19
Sub-bituminous FA; 5/95	0.10	0.053	0.039	0.19

Table 32. External dose three quarters across room (mSv y^{-1}), occupancy of 100%, adult male, 10x12x8 ft^3.

Type; FA%/Concrete%	^{238}U	^{232}Th	^{40}K	Total
Bituminous FA; 25/75	0.52	0.26	0.17	0.95
Sub-bituminous FA; 25/75	0.51	0.28	0.13	0.92
Concrete; 0/100	0.36	0.20	0.15	0.72
Bituminous FA; 15/85	0.46	0.24	0.16	0.86
Sub-bituminous FA; 15/85	0.45	0.25	0.14	0.84
Bituminous FA; 5/95	0.40	0.21	0.16	0.77
Sub-bituminous FA; 5/95	0.39	0.22	0.15	0.76

Table 33. External dose three quarters across room (mSv y^{-1}), occupancy of 65%, adult male, 10x12x8 ft^3.

Type; FA%/Concrete%	^{238}U	^{232}Th	^{40}K	Total
Bituminous FA; 25/75	0.23	0.13	0.10	0.47
Sub-bituminous; 25/75	0.34	0.17	0.11	0.62
Concrete; 0/100	0.33	0.18	0.085	0.59
Bituminous FA; 15/85	0.30	0.16	0.11	0.56
Sub-bituminous FA; 15/85	0.30	0.16	0.091	0.55
Bituminous FA; 5/95	0.26	0.14	0.10	0.50
Sub-bituminous FA; 5/95	0.26	0.14	0.10	0.49

Table 34. External dose three quarters across room (mSv y^{-1}), occupancy of 25%, adult male, 10x12x8 ft^3.

Type; FA%/Concrete%	^{238}U	^{232}Th	^{40}K	Total
Bituminous FA; 25/75	0.09	0.050	0.039	0.18
Sub-bituminous; 25/75	0.13	0.066	0.042	0.24
Concrete; 0/100	0.13	0.069	0.033	0.23
Bituminous FA; 15/85	0.12	0.060	0.041	0.22
Sub-bituminous FA; 15/85	0.11	0.062	0.035	0.21
Bituminous FA; 5/95	0.10	0.054	0.039	0.19
Sub-bituminous FA; 5/95	0.10	0.054	0.037	0.19

Cumulative dose for male, female and child (male 10 years old)

Table 35. Total dose (mSv y^{-1}), occupancy of 100%, adult male.

Type; FA%/Concrete%	Room size	Internal	External	Total
Bituminous FA; 25/75	6x12x8 ft^3	0.26	0.92	1.18
	10x12x8 ft^3	0.21	0.96	1.17
	12x15x8 ft^3	0.19	0.94	1.13
Sub-bituminous; 25/75	6x12x8 ft^3	0.25	0.89	1.14
	10x12x8 ft^3	0.21	0.93	1.14
	12x15x8 ft^3	0.19	0.90	1.09
Concrete; 0/100	6x12x8 ft^3	0.19	0.70	0.89
	10x12x8 ft^3	0.15	0.73	0.88
	12x15x8 ft^3	0.14	0.71	0.85
Bituminous FA; 15/85	6x12x8 ft^3	0.23	0.84	1.07
	10x12x8 ft^3	0.19	0.88	1.07
	12x15x8 ft^3	0.17	0.86	1.03
Sub-bituminous FA; 15/85	6x12x8 ft^3	0.23	0.82	1.05
	10x12x8 ft^3	0.19	0.86	1.05
	12x15x8 ft^3	0.17	0.83	1.00
Bituminous FA; 5/95	6x12x8 ft^3	0.20	0.75	0.95
	10x12x8 ft^3	0.17	0.78	0.95
	12x15x8 ft^3	0.15	0.76	0.91
Sub-bituminous FA; 5/95	6x12x8 ft^3	0.20	0.74	0.94
	10x12x8 ft^3	0.17	0.77	0.94
	12x15x8 ft^3	0.15	0.76	0.91

Table 36. Total dose (mSv y^{-1}), occupancy of 65%, adult male.

Type	Room size	Internal	External	Total
Bituminous FA; 25/75	6x12x8 ft^3	0.17	0.60	0.77
	10x12x8 ft^3	0.14	0.62	0.76
	12x15x8 ft^3	0.12	0.61	0.73
Sub-bituminous; 25/75	6x12x8 ft^3	0.16	0.58	0.74
	10x12x8 ft^3	0.14	0.60	0.74
	12x15x8 ft^3	0.12	0.59	0.71
Concrete; 0/100	6x12x8 ft^3	0.12	0.45	0.57
	10x12x8 ft^3	0.10	0.47	0.57
	12x15x8 ft^3	0.09	0.46	0.55
Bituminous FA; 15/85	6x12x8 ft^3	0.15	0.55	0.70
	10x12x8 ft^3	0.12	0.57	0.69
	12x15x8 ft^3	0.11	0.56	0.67
Sub-bituminous FA; 15/85	6x12x8 ft^3	0.15	0.53	0.68
	10x12x8 ft^3	0.12	0.56	0.68
	12x15x8 ft^3	0.11	0.54	0.65
Bituminous FA; 5/95	6x12x8 ft^3	0.13	0.49	0.62
	10x12x8 ft^3	0.11	0.51	0.62
	12x15x8 ft^3	0.10	0.50	0.60
Sub-bituminous FA; 5/95	6x12x8 ft^3	0.13	0.48	0.61
	10x12x8 ft^3	0.11	0.50	0.61
	12x15x8 ft^3	0.10	0.49	0.59

Table 37. Total dose (mSv y^{-1}), occupancy of 25%, adult male.

Type	Room size	Internal	External	Total
Bituminous FA; 25/75	6x12x8 ft^3	0.064	0.23	0.29
	10x12x8 ft^3	0.053	0.24	0.29
	12x15x8 ft^3	0.047	0.23	0.28
Sub-bituminous; 25/75	6x12x8 ft^3	0.063	0.22	0.28
	10x12x8 ft^3	0.052	0.23	0.28
	12x15x8 ft^3	0.046	0.23	0.28
Concrete; 0/100	6x12x8 ft^3	0.047	0.17	0.22
	10x12x8 ft^3	0.038	0.18	0.22
	12x15x8 ft^3	0.034	0.18	0.21
Bituminous FA; 15/85	6x12x8 ft^3	0.058	0.21	0.27
	10x12x8 ft^3	0.047	0.22	0.27
	12x15x8 ft^3	0.042	0.21	0.25
Sub-bituminous FA; 15/85	6x12x8 ft^3	0.057	0.21	0.27
	10x12x8 ft^3	0.047	0.21	0.26
	12x15x8 ft^3	0.042	0.21	0.25
Bituminous FA; 5/95	6x12x8 ft^3	0.051	0.19	0.24
	10x12x8 ft^3	0.042	0.19	0.23
	12x15x8 ft^3	0.037	0.19	0.23
Sub-bituminous FA; 5/95	6x12x8 ft^3	0.050	0.19	0.24
	10x12x8 ft^3	0.041	0.19	0.23
	12x15x8 ft^3	0.037	0.19	0.23

Table 38. Total dose (mSv y^{-1}), occupancy of 100%, adult female.

Type; FA%/Concrete%	Room size	Internal	External	Total
Bituminous FA; 25/75	6x12x8 ft^3	0.26	1.10	1.36
	10x12x8 ft^3	0.21	1.12	1.33
	12x15x8 ft^3	0.19	1.10	1.29
Sub-bituminous; 25/75	6x12x8 ft^3	0.25	1.06	1.31
	10x12x8 ft^3	0.21	1.08	1.29
	12x15x8 ft^3	0.19	1.06	1.25
Concrete; 0/100	6x12x8 ft^3	0.19	0.83	1.02
	10x12x8 ft^3	0.15	0.85	1.00
	12x15x8 ft^3	0.14	0.83	0.97
Bituminous FA; 15/85	6x12x8 ft^3	0.23	1.01	1.24
	10x12x8 ft^3	0.19	1.02	1.21
	12x15x8 ft^3	0.17	1.00	1.17
Sub-bituminous FA; 15/85	6x12x8 ft^3	0.23	0.98	1.21
	10x12x8 ft^3	0.19	0.99	1.18
	12x15x8 ft^3	0.17	0.98	1.15
Bituminous FA; 5/95	6x12x8 ft^3	0.20	0.90	1.10
	10x12x8 ft^3	0.17	0.91	1.08
	12x15x8 ft^3	0.15	0.89	1.04
Sub-bituminous FA; 5/95	6x12x8 ft^3	0.20	0.89	1.09
	10x12x8 ft^3	0.17	0.90	1.07
	12x15x8 ft^3	0.15	0.88	1.03

Table 39. Total dose (mSv y^{-1}), occupancy of 65%, adult female.

Type	Room size	Internal	External	Total
Bituminous FA; 25/75	6x12x8 ft^3	0.17	0.72	0.89
	10x12x8 ft^3	0.14	0.72	0.86
	12x15x8 ft^3	0.12	0.71	0.83
Sub-bituminous; 25/75	6x12x8 ft^3	0.16	0.69	0.85
	10x12x8 ft^3	0.14	0.7	0.84
	12x15x8 ft^3	0.12	0.69	0.81
Concrete; 0/100	6x12x8 ft^3	0.12	0.54	0.66
	10x12x8 ft^3	0.10	0.55	0.65
	12x15x8 ft^3	0.09	0.54	0.63
Bituminous FA; 15/85	6x12x8 ft^3	0.15	0.65	0.80
	10x12x8 ft^3	0.12	0.66	0.78
	12x15x8 ft^3	0.11	0.65	0.76
Sub-bituminous FA; 15/85	6x12x8 ft^3	0.15	0.64	0.79
	10x12x8 ft^3	0.12	0.65	0.77
	12x15x8 ft^3	0.11	0.64	0.75
Bituminous FA; 5/95	6x12x8 ft^3	0.13	0.58	0.71
	10x12x8 ft^3	0.11	0.59	0.70
	12x15x8 ft^3	0.10	0.58	0.68
Sub-bituminous FA; 5/95	6x12x8 ft^3	0.13	0.58	0.71
	10x12x8 ft^3	0.11	0.58	0.69
	12x15x8 ft^3	0.10	0.58	0.68

Table 40. Total dose (mSv y^{-1}), occupancy of 25%, adult female.

Type	Room size	Internal	External	Total
Bituminous FA; 25/75	6x12x8 ft^3	0.064	0.28	0.34
	10x12x8 ft^3	0.053	0.28	0.33
	12x15x8 ft^3	0.047	0.27	0.32
Sub-bituminous; 25/75	6x12x8 ft^3	0.063	0.27	0.33
	10x12x8 ft^3	0.052	0.27	0.32
	12x15x8 ft^3	0.046	0.26	0.31
Concrete; 0/100	6x12x8 ft^3	0.047	0.21	0.26
	10x12x8 ft^3	0.038	0.21	0.25
	12x15x8 ft^3	0.034	0.21	0.24
Bituminous FA; 15/85	6x12x8 ft^3	0.058	0.25	0.31
	10x12x8 ft^3	0.047	0.25	0.30
	12x15x8 ft^3	0.042	0.25	0.29
Sub-bituminous FA; 15/85	6x12x8 ft^3	0.057	0.25	0.31
	10x12x8 ft^3	0.047	0.25	0.30
	12x15x8 ft^3	0.042	0.24	0.28
Bituminous FA; 5/95	6x12x8 ft^3	0.051	0.22	0.27
	10x12x8 ft^3	0.042	0.23	0.27
	12x15x8 ft^3	0.037	0.22	0.26
Sub-bituminous FA; 5/95	6x12x8 ft^3	0.050	0.22	0.27
	10x12x8 ft^3	0.041	0.22	0.26
	12x15x8 ft^3	0.037	0.22	0.26

Table 41. Total dose (mSv y^{-1}), occupancy of 100%, 10 year old male.

Type; FA%/Concrete%	Room size	Internal	External	Total
Bituminous FA; 25/75	6x12x8 ft^3	0.26	1.05	1.31
	10x12x8 ft^3	0.21	1.08	1.29
	12x15x8 ft^3	0.19	1.06	1.25
Sub-bituminous; 25/75	6x12x8 ft^3	0.25	1.02	1.27
	10x12x8 ft^3	0.21	1.05	1.26
	12x15x8 ft^3	0.19	1.02	1.21
Concrete; 0/100	6x12x8 ft^3	0.19	0.80	0.99
	10x12x8 ft^3	0.15	0.82	0.97
	12x15x8 ft^3	0.14	0.81	0.95
Bituminous FA; 15/85	6x12x8 ft^3	0.23	0.91	1.14
	10x12x8 ft^3	0.19	0.99	1.18
	12x15x8 ft^3	0.17	0.97	1.14
Sub-bituminous FA; 15/85	6x12x8 ft^3	0.23	0.94	1.17
	10x12x8 ft^3	0.19	0.91	1.10
	12x15x8 ft^3	0.17	0.95	1.12
Bituminous FA; 5/95	6x12x8 ft^3	0.20	0.86	1.06
	10x12x8 ft^3	0.17	0.88	1.05
	12x15x8 ft^3	0.15	0.87	1.02
Sub-bituminous FA; 5/95	6x12x8 ft^3	0.20	0.85	1.05
	10x12x8 ft^3	0.17	0.87	1.04
	12x15x8 ft^3	0.15	0.86	1.01

Table 42. Total dose (mSv y^{-1}), occupancy of 65%, 10 year old male.

Type	Room size	Internal	External	Total
Bituminous FA; 25/75	6x12x8 ft^3	0.17	0.68	0.85
	10x12x8 ft^3	0.14	0.70	0.84
	12x15x8 ft^3	0.12	0.69	0.81
Sub-bituminous; 25/75	6x12x8 ft^3	0.16	0.66	0.82
	10x12x8 ft^3	0.14	0.68	0.82
	12x15x8 ft^3	0.12	0.66	0.78
Concrete; 0/100	6x12x8 ft^3	0.12	0.52	0.64
	10x12x8 ft^3	0.10	0.53	0.63
	12x15x8 ft^3	0.09	0.53	0.62
Bituminous FA; 15/85	6x12x8 ft^3	0.15	0.59	0.74
	10x12x8 ft^3	0.12	0.64	0.76
	12x15x8 ft^3	0.11	0.63	0.74
Sub-bituminous FA; 15/85	6x12x8 ft^3	0.15	0.61	0.76
	10x12x8 ft^3	0.12	0.59	0.71
	12x15x8 ft^3	0.11	0.61	0.72
Bituminous FA; 5/95	6x12x8 ft^3	0.13	0.56	0.69
	10x12x8 ft^3	0.11	0.57	0.68
	12x15x8 ft^3	0.10	0.56	0.66
Sub-bituminous FA; 5/95	6x12x8 ft^3	0.13	0.55	0.68
	10x12x8 ft^3	0.11	0.57	0.68
	12x15x8 ft^3	0.10	0.56	0.66

Table 43. Total dose (mSv y^{-1}), occupancy of 25%, 10 year old male.

Type	Room size	Internal	External	Total
Bituminous FA; 25/75	6x12x8 ft^3	0.064	0.26	0.32
	10x12x8 ft^3	0.053	0.27	0.32
	12x15x8 ft^3	0.047	0.27	0.32
Sub-bituminous; 25/75	6x12x8 ft^3	0.063	0.25	0.31
	10x12x8 ft^3	0.052	0.26	0.31
	12x15x8 ft^3	0.046	0.25	0.30
Concrete; 0/100	6x12x8 ft^3	0.047	0.2	0.25
	10x12x8 ft^3	0.038	0.2	0.24
	12x15x8 ft^3	0.034	0.2	0.23
Bituminous FA; 15/85	6x12x8 ft^3	0.058	0.23	0.29
	10x12x8 ft^3	0.047	0.25	0.30
	12x15x8 ft^3	0.042	0.24	0.28
Sub-bituminous FA; 15/85	6x12x8 ft^3	0.057	0.23	0.29
	10x12x8 ft^3	0.047	0.23	0.28
	12x15x8 ft^3	0.042	0.24	0.28
Bituminous FA; 5/95	6x12x8 ft^3	0.051	0.21	0.26
	10x12x8 ft^3	0.042	0.22	0.26
	12x15x8 ft^3	0.037	0.22	0.26
Sub-bituminous FA; 5/95	6x12x8 ft^3	0.050	0.21	0.26
	10x12x8 ft^3	0.041	0.22	0.26
	12x15x8 ft^3	0.037	0.21	0.25

Comparison results

Table 44. Total dose (mSv y^{-1}), occupancy of 100%.

Type; FA%/Concrete%	Room size	Male	Female	Child
Bituminous FA; 25/75	6x12x8 ft^3	1.18	1.36	1.31
	10x12x8 ft^3	1.17	1.33	1.29
	12x15x8 ft^3	1.13	1.29	1.25
Sub-bituminous; 25/75	6x12x8 ft^3	1.14	1.31	1.27
	10x12x8 ft^3	1.14	1.29	1.26
	12x15x8 ft^3	1.09	1.25	1.21
Concrete; 0/100	6x12x8 ft^3	0.89	1.02	0.99
	10x12x8 ft^3	0.88	1.00	0.97
	12x15x8 ft^3	0.85	0.97	0.95
Bituminous FA; 15/85	6x12x8 ft^3	1.07	1.24	1.14
	10x12x8 ft^3	1.07	1.21	1.18
	12x15x8 ft^3	1.03	1.17	1.14
Sub-bituminous FA; 15/85	6x12x8 ft^3	1.05	1.21	1.17
	10x12x8 ft^3	1.05	1.18	1.10
	12x15x8 ft^3	1.00	1.15	1.12
Bituminous FA; 5/95	6x12x8 ft^3	0.95	1.10	1.06
	10x12x8 ft^3	0.95	1.08	1.05
	12x15x8 ft^3	0.91	1.04	1.02
Sub-bituminous FA; 5/95	6x12x8 ft^3	0.94	1.09	1.05
	10x12x8 ft^3	0.94	1.07	1.04
	12x15x8 ft^3	0.91	1.03	1.01

Table 45. Total dose (mSv y^{-1}), occupancy of 65%.

Type; FA%/Concrete%	Room size	Male	Female	Child
Bituminous FA; 25/75	6x12x8 ft^3	0.77	0.89	0.85
	10x12x8 ft^3	0.76	0.86	0.84
	12x15x8 ft^3	0.73	0.83	0.81
Sub-bituminous; 25/75	6x12x8 ft^3	0.74	0.85	0.82
	10x12x8 ft^3	0.74	0.84	0.82
	12x15x8 ft^3	0.71	0.81	0.78
Concrete; 0/100	6x12x8 ft^3	0.57	0.66	0.64
	10x12x8 ft^3	0.57	0.65	0.63
	12x15x8 ft^3	0.55	0.63	0.62
Bituminous FA; 15/85	6x12x8 ft^3	0.70	0.80	0.74
	10x12x8 ft^3	0.69	0.78	0.76
	12x15x8 ft^3	0.67	0.76	0.74
Sub-bituminous FA; 15/85	6x12x8 ft^3	0.68	0.79	0.76
	10x12x8 ft^3	0.68	0.77	0.71
	12x15x8 ft^3	0.65	0.75	0.72
Bituminous FA; 5/95	6x12x8 ft^3	0.62	0.71	0.69
	10x12x8 ft^3	0.62	0.70	0.68
	12x15x8 ft^3	0.60	0.68	0.66
Sub-bituminous FA; 5/95	6x12x8 ft^3	0.61	0.71	0.68
	10x12x8 ft^3	0.61	0.69	0.68
	12x15x8 ft^3	0.59	0.68	0.66

Table 46. Total dose (mSv y^{-1}), occupancy of 25%.

Type; FA%/Concrete%	Room size	Male	Female	Child
Bituminous FA; 25/75	6x12x8 ft^3	0.29	0.34	0.32
	10x12x8 ft^3	0.29	0.33	0.32
	12x15x8 ft^3	0.28	0.32	0.32
Sub-bituminous; 25/75	6x12x8 ft^3	0.28	0.33	0.31
	10x12x8 ft^3	0.28	0.32	0.31
	12x15x8 ft^3	0.28	0.31	0.30
Concrete; 0/100	6x12x8 ft^3	0.22	0.26	0.25
	10x12x8 ft^3	0.22	0.25	0.24
	12x15x8 ft^3	0.21	0.24	0.23
Bituminous FA; 15/85	6x12x8 ft^3	0.27	0.31	0.29
	10x12x8 ft^3	0.27	0.30	0.30
	12x15x8 ft^3	0.25	0.29	0.28
Sub-bituminous FA; 15/85	6x12x8 ft^3	0.27	0.31	0.29
	10x12x8 ft^3	0.26	0.30	0.28
	12x15x8 ft^3	0.25	0.28	0.28
Bituminous FA; 5/95	6x12x8 ft^3	0.24	0.27	0.26
	10x12x8 ft^3	0.23	0.27	0.26
	12x15x8 ft^3	0.23	0.26	0.26
Sub-bituminous FA; 5/95	6x12x8 ft^3	0.24	0.27	0.26
	10x12x8 ft^3	0.23	0.26	0.26
	12x15x8 ft^3	0.23	0.26	0.25

Table 47. External dose with center room offset (mSv y^{-1}), occupancy of 100%, adult male, 10x12x8 ft^3.

Type; FA%/Concrete%	Middle	Halfway	Three quarters
Bituminous FA; 25/75	0.96	0.95	0.95
Sub-bituminous; 25/75	0.93	0.92	0.92
Concrete; 0/100	0.73	0.72	0.72
Bituminous FA; 15/85	0.88	0.87	0.86
Sub-bituminous FA; 15/85	0.86	0.85	0.84
Bituminous FA; 5/95	0.78	0.77	0.77
Sub-bituminous FA; 5/95	0.77	0.77	0.76

Table 48. External dose with center room offset (mSv y^{-1}), occupancy of 65%, adult male, 10x12x8 ft^3.

Type; FA%/Concrete%	Middle	Halfway	Three quarters
Bituminous FA; 25/75	0.62	0.62	0.62
Sub-bituminous; 25/75	0.60	0.60	0.60
Concrete; 0/100	0.47	0.47	0.47
Bituminous FA; 15/85	0.57	0.57	0.56
Sub-bituminous FA; 15/85	0.56	0.55	0.55
Bituminous FA; 5/95	0.51	0.50	0.50
Sub-bituminous FA; 5/95	0.50	0.50	0.49

Table 49. External dose with center room offset (mSv y^{-1}), occupancy of 25%, adult male, 10x12x8 ft^3.

Type; FA%/Concrete%	Middle	Halfway	Three quarters
Bituminous FA; 25/75	0.24	0.24	0.24
Sub-bituminous; 25/75	0.23	0.23	0.23
Concrete; 0/100	0.18	0.18	0.18
Bituminous FA; 15/85	0.22	0.22	0.22
Sub-bituminous FA; 15/85	0.21	0.21	0.21
Bituminous FA; 5/95	0.19	0.19	0.19
Sub-bituminous FA; 5/95	0.19	0.19	0.19

CHAPTER V

DISCUSSION

Specific activity analysis

^{238}U concentrations in bituminous fly ash samples varied from 30 to 217 Bq kg^{-1} (119 ± 45 Bq kg^{-1}) (all values in parentheses mean ± 1 s.d), and concentrations in sub-bituminous fly ash samples varied from 72 to 209 Bq kg^{-1} (115 ± 40 Bq kg^{-1}); ^{232}Th concentrations in bituminous fly ash samples varied from 10 to 120 Bq kg^{-1} (73 ± 26 Bq kg^{-1}), and concentrations in sub-bituminous fly ash samples varied from 53 to 110 Bq kg^{-1} (81 ± 18 Bq kg^{-1}); ^{40}K concentrations in bituminous fly ash samples varied from 177 to 928 Bq kg^{-1} (569 ± 184 Bq kg^{-1}), and in sub-bituminous fly ash samples varied from 87 to 303 Bq kg^{-1} (171 ± 69 Bq kg^{-1}). Fly ash specific activities found in this study are relatively consistent with those of other authors (Coles et al. 1978, Papastefanou 2010, Turhan et al. 2010), but were overall somewhat on the low side of their reported ranges, although means were similar. The variability in our samples was less than that observed in the literature, but the literature values encompassed many kinds of samples, both from domestic and international sources, while our samples were all from within the United States. The specific activities of the fly ash were similar to other building materials such as stones, rocks and cement (NCRP 1987). The mean specific activities were slightly higher than the world average of building materials, with ^{238}U, ^{232}Th and ^{40}K having 50, 50 and 500 Bq kg^{-1} respectively (UNSCEAR 1993).

FGD gypsum specific activities were much lower, with many below system MDAs, even with 72 hour counting times. Concentrations varied from 1 to 24 Bq kg^{-1} (9 ± 5 Bq kg^{-1}); from below MDA to 3 Bq kg^{-1} (1 ± 1 Bq kg^{-1}); from below MDA to 19 Bq kg^{-1} (10 ± 5 Bq kg^{-1}). The concentrations in scrubber sludge samples varied from 0.2 to 174 Bq kg^{-1} (58 ± 58 Bq kg^{-1}); from below MDA to 85 Bq kg^{-1} (22 ± 28 Bq kg^{-1}); from 9 to 541 Bq kg^{-1} (164 ± 165 Bq kg^{-1}) for ^{238}U, ^{232}Th and ^{40}K respectively.

Bituminous and sub-bituminous fly ashes are very similar in specific activity for ^{238}U and ^{232}Th; however, ^{40}K specific activity values were approximately three times higher than in bituminous fly ash samples. FGD gypsum sample concentrations are comparable to those from natural gypsum samples and are an order of magnitude lower than in fly ash samples. Natural gypsum samples, along with FGD gypsum samples, have much lower specific activity levels, as found in our measurements and reported by others (El Afifi et al. 2006, Trevisi et al. 2012), and appear to be negligible dose contributors for use in dose and risk assessment from their use in building materials. Scrubber sludge concentrations were lower than those in fly ash samples, but the range was wide because the composition of sludge samples can be quite variable. Thus, overall, our values were quite comparable to what others have found in similar sample types.

Headspace analysis

The headspace analysis was performed for both types of fly ash, and averages were calculated using both the containers with headspace and smaller petri dishes. Averages for the polypropylene jars and the petri dishes were 118 and 144 Bq kg^{-1}; 75 and 89 Bq kg^{-1}; 477 and 606 Bq kg^{-1} for ^{238}U, ^{232}Th and ^{40}K respectively. The ratios of the concentrations in the petri

dishes to those in the jars were 1.28, 1.38 and 1.27 for ^{238}U, ^{232}Th and ^{40}K. If radon and thoron

gas was escaping through the headspace in such a way as to alter the counting efficiency, the

results would have shown an increase in specific activity for both ^{238}U and ^{232}Th but not for ^{40}K.

Due to the equal increase in concentration of ^{40}K, an alternative explanation is necessary other

than the escape of radon/thoron gas was causing the change in counting efficiency seen in the

smaller petri dishes. A 3 mm layer of material was found present at the bottom of the

polypropylene jars that was not present in the petri dishes. It was concluded that the

separation of the sample from the detector due to this layer of material was causing a slight

change in counting efficiency from use of Petri dishes. Since the detector was calibrated using a

standard with the same type of polypropylene jars (with the 3 mm base), the correct specific

activity of the samples were based on the results obtained from the larger containers.

Radon internal dose analysis

It was assumed that 25% fly ash was the maximum concentration that would be used in

building materials, which is the maximum allowable be the American Concrete Institute (ACI

2005). The radon dose changed from 0.19 to 0.26 mSv y^{-1} for a 6x12x8 ft^3 room, 0.15 to 0.21

mSv y^{-1} for a 10x12x8 ft^3, 0.14 to 0.19 mSv y^{-1} for a 15x12x8 ft^3 when a 25% fly ash

concentration was assumed, instead of pure concrete.   This gives an increased dose of 0.07,

0.06 and 0.05 mSv y^{-1} when a person is in a 25%/75% room instead of in a pure concrete room.

This is small compared to the annual limit of the public, 1 mSv y^{-1} (10CFR20 1997). This is also

assuming occupancy of 100%, which is unrealistic for the average person. UNSCEAR (2000)

estimated the world's population of radon and thoron dose to be 1.275 mSv y^{-1} and an increase

of a maximum of 0.07 mSv y^{-1} is small compared to the total dose received by the average person. The maximum indoor radon concentration, 10.29 Bq m^3, is also well below the maximum of 100 Bq m^3 advised by the World Health Organization (WHO 2009).   The results, as expected, gave highest doses in the smallest rooms. This is confirmed by similar literature (Sathish et. al 2011).

Radon dose was assumed to be relatively the same for both sexes; age-dependent models were not found in the literature. Though the breathing rate is most likely slightly different for male and female, it might differ quite a bit for a child compared to an adult; however tidal volumes are smaller and this may offset the effect of higher breathing rates somewhat.

The fly ash percentages for this study were presumed to be 25% and 15% of concrete, however, typical mass percentages are usually around 2-3% with a high loading of 6%. This means that 20-45% of cement will be substituted for fly ash. Doses in this study will accordingly be higher than in actuality.

Monte Carlo external dose analysis

The male adult external dose with 100% occupancy varied from 0.92 to 0.7 mSv y^{-1} for a 6x12x8 ft^3 room, 0.96 to 0.73 mSv y^{-1} for a 10x12x8 ft^3 room, 0.94 to 0.71 mSv y^{-1} for a 15x12x8 ft^3 room, for rooms with 25%/75% fly ash and concrete mixture to 0%/100% pure concrete. The female adult external dose with 100% occupancy varied from 1.10 to 0.83 mSv y^{-1} for a 6x12x8 ft^3 room, 1.12 to 0.85 mSv y^{-1} for a 10x12x8 ft^3 room, 1.10 to 0.83 mSv y^{-1} for a 15x12x8 ft^3 room, for rooms with 25%/75% fly ash and concrete mixture to 0%/100% pure concrete.

The male child of ten years old external dose with 100% occupancy varied from 1.05 to 0.8 mSv y^{-1} for a 6x12x8 ft^3 room, 1.08 to 0.82 mSv y^{-1} for a 10x12x8 ft^3 room, 1.06 to 0.81 mSv y^{-1} for a 15x12x8 ft^3 room, for rooms with 25%/75% fly ash and concrete mixture to 0%/100% pure concrete. The male adult external dose with 100% occupancy and a room size of 10x12x8 ft^3 varied from 0.95 to 0.72 mSv y^{-1} for a center offset of halfway across the room and 0.95 to 0.72 mSv y^{-1} for a center offset of three quarters across the room.

In general, doses per Bq in the walls are higher for smaller rooms, but this is offset by the overall higher amounts of total activity in larger rooms (i.e. due to more kg of concrete); thus there is no clear pattern for doses as the volume of the room increases. The results show that the 10x12x8 ft^3 volume room had a higher dose of the other two, so the multiplication of the decreasing volume of concrete with the increasing Sv per disintegration was the determining factor, and the dose was not significantly different from the room sizes. Female dose is the highest, due to the radiosensitivity of the breast tissue, for which males do not have. The male child had the next highest dose, level the male adult with the least amount of dose. Since both the adult and child are assumed to have the same tissue weighting factors (ICRP 103) the dose just depends on differences in body size. The difference in weight translates to a higher dose in Sv, which is the only factor different in the calculation for annual dose; however with external dose, fewer photons are intercepted by a smaller individual. The doses calculated for the center, halfway center offset and three-fourths offset were not different; it appears that dose reductions due to distance from one wall are offset by proximity to the other.

Internal and external total dose analysis

The male adult total dose with 100% occupancy varied from 1.18 to 0.89 mSv y^{-1} for a 6x12x8 ft^3, room 1.17 to 0.88 mSv y^{-1} for a 10x12x8 ft^3 room, 1.13 to 0.85 mSv y^{-1} for a 15x12x8 ft^3 room, for rooms with 25%/75% fly ash and concrete mixture to 0%/100% pure concrete. The female adult total dose with 100% occupancy varied from 1.36 to 1.02 mSv y^{-1} for a 6x12x8 ft^3 room, 1.33 to 1.00 mSv y^{-1} for a 10x12x8 ft^3 room, 1.29 to 0.97 mSv y^{-1} for a 15x12x8 ft^3 room, for rooms with 25%/75% fly ash and concrete mixture to 0%/100% pure concrete. The male child of ten years old total dose with 100% occupancy varied from 1.31 to 0.99 mSv y^{-1} for a 6x12x8 ft^3 room, 1.29 to 0.97 mSv y^{-1} for a 10x12x8 ft^3 room, 1.25 to 0.97 mSv y^{-1} for a 15x12x8 ft^3 room, for rooms with 25%/75% fly ash and concrete mixture to 0%/100% pure concrete. The percent differences between women vs man, woman vs child, and child vs man were on an average of 14, 3.4, and 11 percent, respectively, assuming full occupancy.

The average annual dose received by natural sources is 2.4 mSv, with 1.26 mSv received from radon and 0.48 from external terrestrial radiation (UNSCEAR 2000). This indicates that our radon dose may be underestimated, while our external dose could be overestimated. Overall, however, the doses suggest that even at maximum occupation this is not more than the world average of 2.4 mSv y^{-1} (UNSCEAR 2000). It is also unknown that doses so low can lead to cancer. Although many accept the tenets of the 'linear no threshold' (LNT) model of radiation carcinogenesis, others dispute its applicability at low doses and dose rates. The BEIR VII Committee (BEIR VII 2006) found that cancer risks were 'not inconsistent' with a LNT model, while the French Academy of the Sciences concluded that there was not enough evidence to extrapolate cancer risks from high doses and dose rates to lower values (Aurengo et al. 2005).

Other theories hold that doses below 100 mGy of radiation could even produce a protective effect ('hormesis') by stimulating cellular repair mechanisms (Cameron and Moulder 1998). At present it is unknown what doses may poses a threat to human health (Feinendegen 2005). The theoretical doses calculated in this work, from the possible inclusion of fly ash material into building materials are very low, and within the variability of natural background rates in the US. In Figure 28 it is shown the variability of the natural background in the US (Dixon 2007).
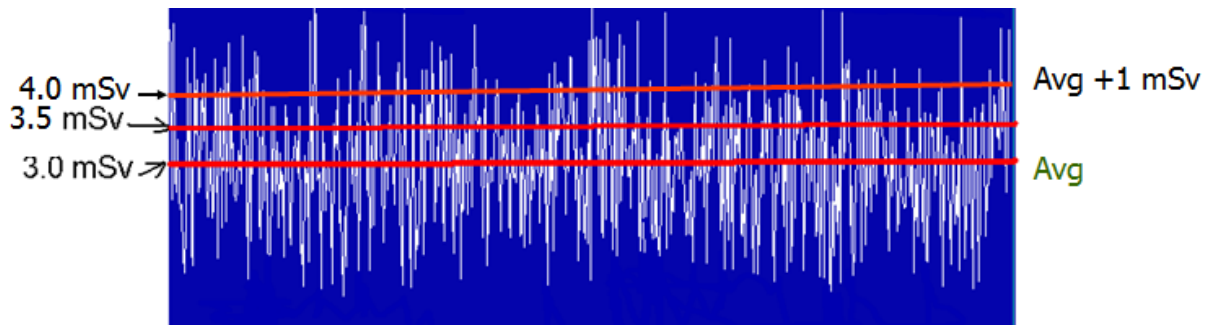

Figure 28. Variability of the natural radiation background in the US.

Indeed, the variability of natural levels of ^{238}U, ^{232}Th and ^{40}K in concrete (with no fly ash added) is considerable, thus drawing specific conclusions about increased risk of cancer from inclusion of fly ash in building materials is not possible from these data.

Chapter VI

Conclusions

Concentrations of ^{238}U, ^{232}Th and ^{40}K were analyzed in various samples of fly ash, gypsum and other related materials. The concentrations in fly ash were detectable with 8 hour counting times and produced values that were similar to values established in the literature by others. Fly ash bituminous ^{238}U concentrations varied from 30 to 217 Bq kg^{-1} (mean $\pm$ 1 sd 119 $\pm$ 45 Bq kg^{-1}), and sub-bituminous concentrations varied from 72 to 209 Bq kg^{-1} (115 $\pm$ 40 Bq kg^{-1}); bituminous ^{232}Th concentrations varied from 10 to 120 Bq kg^{-1} (73 $\pm$ 26 Bq kg^{-1}), and sub–bituminous concentrations varied from 53 to 110 Bq kg^{-1} (81 $\pm$ 18 Bq kg^{-1}); bituminous ^{40}K concentrations varied from 177 to 928 Bq kg^{-1} (569 $\pm$ 184 Bq kg^{-1}), and sub-bituminous concentrations varied from 87 to 303 Bq kg^{-1} (171 $\pm$ 69 Bq kg^{-1}). Concentrations in gypsum samples were much lower, and many were below system MDAs, even with 72 hour counting times. It was concluded FGD gypsum has negligible amounts of radionuclides and therefore is not a relevant contributor to dose.

Samples were transferred from polypropylene jars into petri dishes to determine if headspace contributed to loss of specific activity due to seepage of radon gas. The headspace analysis used ^{40}K as the control because it did not have a gas component. The ^{40}K specific activity increased almost the same amount as both ^{238}U and ^{232}Th when counted in the petri dishes. It was concluded that this increase was due to the container thickness and not gas escaping through the headspace.

Radon doses were calculated using an equation given by Taylor-Lange et. al 2012. Several factors were variable and chosen based on previous literature. The dose is highly dependent on the air exchange rate and the radon emanation coefficient. For this study, the maximum radon dose was found to be 0.26 mSv y^{-1}, with an occupancy of 100% given the smallest room size.

Monte Carlo simulations were run on Geant4 transport code to estimate external dose. The doses were from highest to lowest for female adult, male child of ten years and male adult. The differences were attributed to differences in weighting factors and weight. For this study, the maximum external dose was found to be 0.96, 1.12, 1.08 mSv y^{-1} for adult male, adult female and 10 year old male, respectively, with an occupancy of 100%.

Total doses estimated from typical levels of these radionuclides in fly ash added to building materials were low, in comparison to routine background, medical and other radiation exposures of the US public, and are within the range of variability of these exposures.

It was concluded the most important factor with respect to eternal dose is occupancy, rather than sex, age or room size, given an upper bound to the usage rate of fly ash in concrete based on construction code requirements. The most important factor with respect to internal dose is occupancy and air exchange rate. Natural materials used in concrete have almost as much naturally occurring radioactivity as the fly ash, so the incremental effect of fly ash usage is small, even with mass percentages as high as 25%.

Eckert & Ziegler

Analytics

1380 Seaboard Industrial Blvd.
Atlanta, Georgia 30318
Tel 404·352·8677
Fax 404·352·2837
www.analyticsinc.com

CERTIFICATE OF CALIBRATION
Standard Radionuclide Source

78179C-465
100 Grams Sand in 250 mL PP MRP Jar

Customer: Vanderbilt University
P.O. No.: MOORE 08-25-08, Item 1
Calibration Date: 01-Jul-2008   12:00 EST   **Grams of Master Source:** 0.011478

This standard radionuclide source was prepared using aliquots measured gravimetrically from master radionuclide solutions. Calibration and purity were checked using a germanium gamma spectrometer system. At the time of calibration no interfering gamma-ray emitting impurities were detected. The gamma-ray emission rates for the most intense gamma-ray lines are given. Analytics maintains traceability to the National Institute of Standards and Technology through a Measurements Assurance Program as described in USNRC Regulatory Guide 4.15, Revision 1, February, 1979, and compliance with ANSI N42.22-1995, "Traceability of Radioactive Sources to NIST."

Nuclide	Gamma-Ray Energy (keV)	Half-Life, Days	Master Source* γps/gram	This Source γps	Uncertainty , % Type u_A	u_B	U	Calibration Method
Am-241	59.5	157860	——	1.450E+03	0.3	1.5	3.1	4π LS
Cd-109	88.0	462.60	1.681E+05	1.929E+03	0.5	1.7	3.5	HPGe
Co-57	122.1	271.79	8.748E+04	1.004E+03	0.6	1.3	2.9	HPGe
Ce-139	165.9	137.6	1.218E+05	1.398E+03	0.6	1.1	2.5	HPGe
Hg-203	279.2	46.61	2.761E+05	3.169E+03	0.6	1.1	2.5	HPGe
Sn-113	391.7	115.1	1.725E+05	1.980E+03	0.7	1.1	2.6	HPGe
Cs-137	661.7	10983	1.078E+05	1.237E+03	0.7	1.2	2.8	HPGe
Y-88	898.0	106.6	4.154E+05	4.768E+03	0.8	1.1	2.7	HPGe
Co-60	1173.2	1925.4	2.017E+05	2.315E+03	0.8	1.1	2.7	HPGe
Co-60	1332.5	1925.4	2.020E+05	2.319E+03	0.6	1.1	2.5	HPGe
Y-88	1836.1	106.6	4.398E+05	5.048E+03	0.7	1.1	2.6	HPGe

* Master Source refers to Analytics' 8-isotope mixture which is calibrated quarterly.

Calibration Methods: 4π LS - 4 pi Liquid Scintillation Counting, HPGe - High Purity Germanium Gamma-Ray Spectrometer, IC - Ionization Chamber. **Uncertainty:** U - Relative expanded uncertainty, k = 2. See NIST Technical Note 1297, "Guidelines for Evaluating and Expressing the Uncertainty of NIST Measurement Results."

Comments:
62.5 mL sand.
This standard will expire one year after the calibration date.

Source Prepared by: _____
N. E. Tibbitts, Radiochemist

QA Approved: _____   QA AT   Date: 9/17/08
D. M. Montgomery, QA Manager

End of Certificate

Corporate Office
24937 Avenue Tibbitts   Valencia, California 91355

Laboratory
1380 Seaboard Industrial Blvd. Atlanta, Georgia, 30318

Figure 29. Certificate of calibration for standard source.

QUALITY ASSURANCE DATA SHEET
GMX SERIES GAMMA-X HPGE
(HIGH-PURITY GERMANIUM) COAXIAL PHOTON DETECTOR SYSTEM

MODEL AND SERIAL NUMBERS

Detector Model No. _GMX 35 P4_

Cryostat Configuration _PopTop_

Dewar Model _—_

Preamplifier Model _A 251N_

Preamplifier S/N _322_

H.V. Filter Model _138EMI_

H.V. Filter S/N _709_

Smart-1-N _—_

Dewar Capacity _—_   Static Holding Time _—_

IMPORTANT REFERENCE DATA

Ship Date _7-6-11_

Serial No. _45-TN12123A_

When calling Customer Service, always reference this Detector Serial No.

Detector Cool-Down Time _—_

DIMENSIONS

Detector Diameter _55.6_ mm

Detector Length _79_ mm

End Cap to Detector _3_ mm

ABSORBING LAYERS

Beryllium _0.50_ mm

Aluminum _—_ mm

Inactive Germanium – 0.3 μm

Recommended Operating Bias, NEGATIVE _4000_ V

PERFORMANCE SPECIFICATIONS*

	Warranted	Measured	Amplifier Time Constant
Resolution (FWHM) at 1.33 MeV, ^{60}Co	2.14 keV	1.89 keV	6 μs
Peak-to-Compton Ratio, ^{60}Co	50:1	56:1	6 μs
Relative Efficiency at 1.33 MeV, ^{60}Co	31.5 %	35.9 %	6 μs
Peak Shape (FWTM/FWHM), ^{60}Co	2.0	1.9	6 μs
Peak Shape (FWFM/FWHM), ^{60}Co		2.8	6 μs
Resolution (FWHM) at 5.9 keV, ^{55}Fe	803 eV	699 eV	6 μs

*Measured at a nominal rate of 1000 counts/s unless otherwise specified.

Other: _Capsule SCA # 7360_

Cryo PV-4 #NA

Data Certified by: _P8 Wilson_   Date: _7-6-11_

Figure 30. QA sheet for Ortec detector.

98

CANBERRA

DETECTOR SPECIFICATIONS AND PERFORMANCE DATA

Specifications

DETECTOR MODEL	BE3830	**SERIAL NUMBER**	10014790
CRYOSTAT MODEL	7500SL	**PREAMPLIFIER MODEL**	2002CSL

The purchase specifications, and therefore the warranted performance, of this detector are as follows:
(Electric cooling may degrade performance by as much as 10%.)

Energy	5.9 keV	122 keV	1332 keV
Resolution [eV (FWHM)]			

Cryostat description (if special) _____

Physical Characteristics

Active diameter	70	mm
Active area	3800	mm^2
Thickness	30	mm
Distance from window	5	mm
Cryostat window thickness	0.6	mm
Cryostat window material	Carbon Composite	

Electrical Characteristics

Depletion voltage _____ (+)2900 _____ V dc
Recommended bias voltage _____ (+)3000 _____ V dc
Reset rate at recommended bias _____ ----- _____ sec (Reset preamp only)
Preamplifier test point voltage at recommended bias _____ (-).22 _____ V dc (RC preamp only)

Resolution and Efficiency

With amp time constant of _____ 4 _____ Microseconds

Isotope	^{55}Fe	^{57}Co	^{57}Co	^{60}Co	Peak to Bkgd.
Energy (keV)	5.9	6.4*	122	1332	
FWHM (eV)	371		611	1762	
FWTM (eV)			1137	3347	

*Substitutes for ^{55}Fe in some cases where ^{55}Fe peaks are not well separated.

Cool Down Time _____ 6 _____ Hours Cryostat Liquid Nitrogen Consumption Rate _____ <1.8 _____ Liters per Day

Tested by: *Wesley Moss* Date: _____ 06/20/07 _____

Approved by: *Stephen Bishop* Date: _____ 06/20/07 _____

800 Research Parkway, Meriden, CT USA 06450 • Tel. 203-238-2351/Fax. 203-639-2420

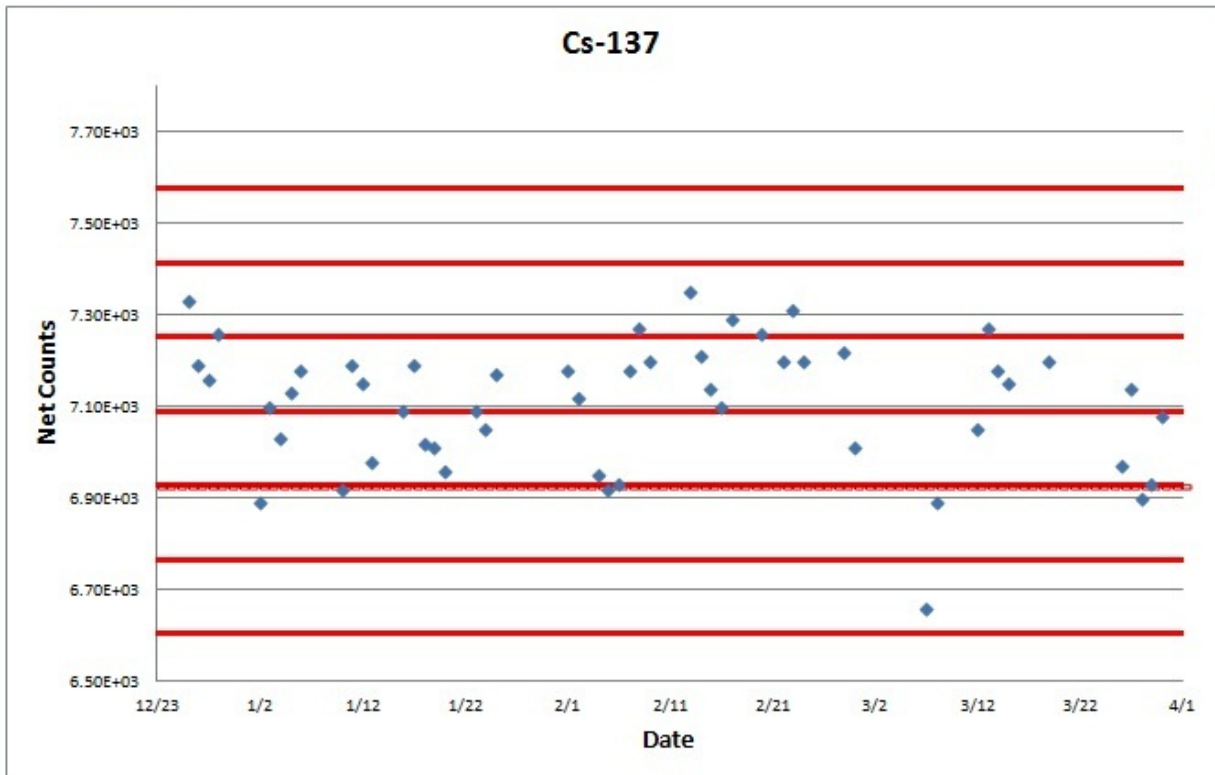Figure 31. Detector specs for Canberra detector.

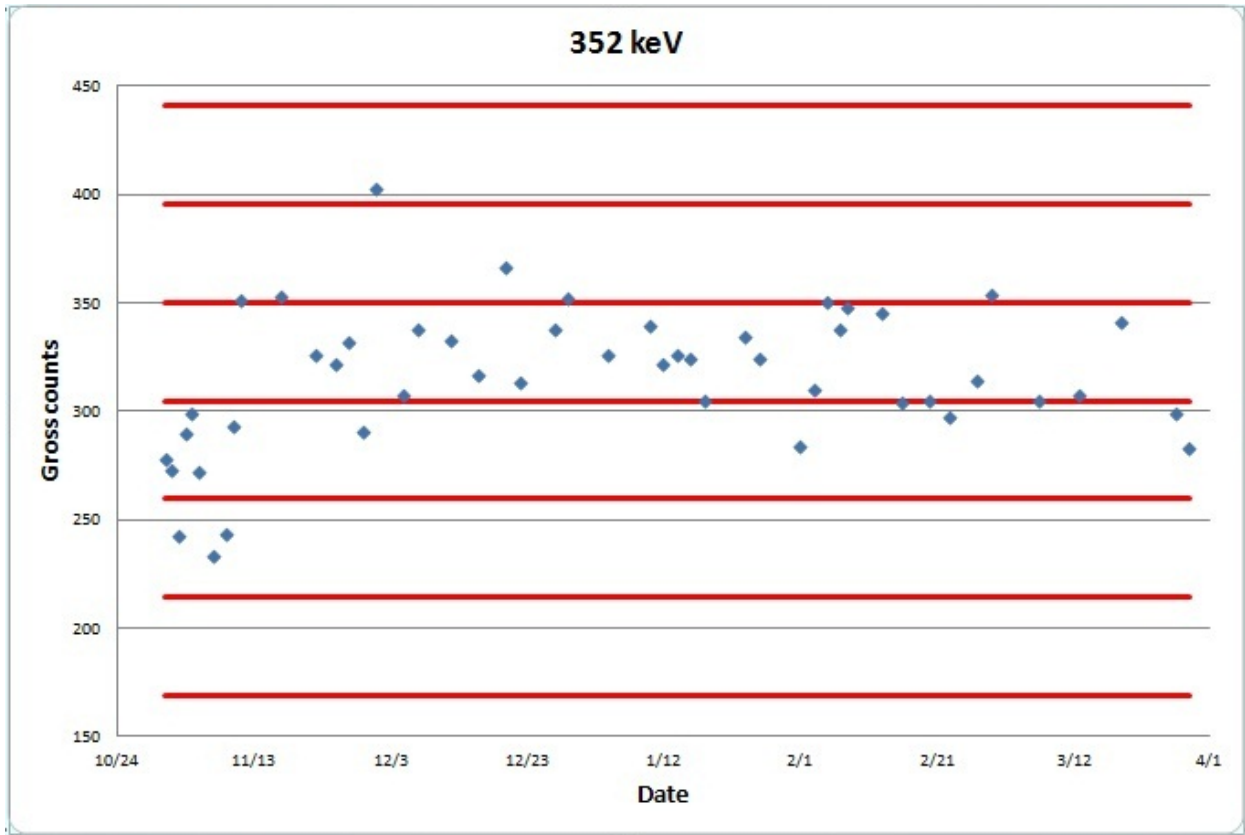Figure 32. Standard Cs-137 QA graph for Canberra detector.

Figure 33. 352 keV background QA graph for Canberra detector.

REFERENCES

ACI. Committee 318, building code requirements for structural concrete (ACI 318-05) and Commentary (ACI 318R-05). Farmington Hills, Michigan: American Concrete Institute; 2005.

Aurengo A, Averbeck D, Bonnin A, Le Guen B, Masse R, Monier R, Tubiana M, Valleron A, Vathaire F. Academy of Sciences - National Academy of Medicine. Dose-effect relationships and estimation of the carcinogenic effects of low doses of ionizing radiation. 2005.

Ackers JG, Denboer JF, de Jong P, Wolschrijn WA. Radioactivity and radon exhalation rates of building materials in the Netherlands. Sci Total Environ 45:151–156; 1985.

Agostinelliae S, Allisonas J, Amako K, et al. Geant4 – A simulation toolkit, *Nuclear Instruments Methods Physics Research A*. 506:250-303; 2003.

American Coal Ash Association. 2010 Coal Combustion Product (CCP) Production & Use Survey Report. 2010.

Amrani D, Tahtat M. Natural radioactivity in Algerian building materials. Appl Radiat Isot 54:687–689; 2001.

Barber DE, Giorgio HR. Gamma-ray activity in bituminous, sub-bituminous and lignite coals. Health Phys 32:83–88; 1977.

Baykal G, Saygili A. A new technique to reduce the radioactivity of fly ash utilized in the construction industry. Fuel 90:1612-1617; 2011.

Beretka J, Mathew PJ. Natural radioactivity of Australian building materials, industrial wastes and by-products. Health Phys 48:87–95; 1985.

Bem H, Wieczorkowski P, Budzanowki M. Evaluation of technologically enhanced natural radiation near the coal-fired power plants in the Lodz region of Poland. J Environmental Radioactivity 61:191-201; 2002.

BEIR VII - Phase 2 Committee Health Risks from Exposure to Low Levels of Ionizing Radiation. Washington, DC: The National Academy Press; 2005.

Briesmeister, J. MCNP – A general Monte Carlo n-particle transport code, version 4B. Los Alamos National Laboratory, report LA-12625-M. 1997.

Brinck WL, Schliekelman RJ, Bennet DL, Bell C, Markwood IM. Radium removal efficiencies in water treatment processes. J Am. Water Works Assoc 70:31-43; 1978.

Brown K. Conceptual Site Model for the Subsurface Disposal Area at the Idaho National Laboratory. 2008.

Cameron JR, Moulder JE. Proposition: radiation hormesis should be elevated to a position of scientific respectability. Med Phys. 25*:1407–1410; 1998.

Canberra. Germanium Detectors: User's Manual. Meriden, CT: Canberra Industries, 1998.

Clarke J. Radioactive Waste Management Overview. Lecture given in PHY 307. 2012.

Code of Federal Regulations. Standards for protection against radiation. 10 Federal Register 20. 2007.

Coles DG, Ragaini RC, Ondov JM. Behavior of natural radionuclides in Western coal-fired power plants. Environmental Science and Technology 12:442-446; 1978.

Currie LA. Limits of qualitative detection and quantitative determination. Analytical Chemistry 40(3):586-593; 1968.

Cole, LA. Element of Risk: The Politics of Radon. AAAS Press, Washington, D.C. 1994.

Coles DG, Ragaini RC, Ondov JM. Behavior of natural radionuclides in Western coal-fired power plants. Environ Science and Technology 12:442-446; 1978.

Dixon, R. Faith-based radiation protection, powerpoint. 2007.

Eisenbud M, Gesell T. Environmental radioactivity: from natural, industrial, and military sources. 4th ed., San Diego, CA: Academic Press, 1997.

El Afifi EM, Hilal MA, Khalifa SM, Aly HF. Evaluation of U, Th, K and emanated radon in some NORM and TENORM samples. Radiation Measurements 41:627-633; 2006.

Environmental Protection Agency. Exposure Factors Handbook: 2011 Edition. EPA/600/R-090/052F; EPA Office of Research and Development. 2011.

Environmental Protection Agency. National primary drinking water regulations, radionuclides; Proposed rule. *Fed. Regist.* 56(No. 138), 33050-33123. 1991.

European Commission. Radiological Protection 112: Radiological Protection Principles concerning the Natural Radioactivity of Building Materials. 1999.

Feinendegen, LE. Evidence for beneficial low level radiation effects and radiation hormesis. British Journal of Radiology. 78:3-7; 2005.

Font J, Casas M, Forteza R, Cerda V, Garcias F. Natural radioactive elements and heavy metals in coal, fly ash and bottom ash from a thermal power plant. J of Environ Science and Health A28:2061–2073; 1993.

Ford RL, Nelson WR. The EGS code system: Computer programmes for Monte Carlo simulation of electromagnetic cascade showers. Report No. SLAC-210, Version 3, Stanford Linear Accelerator Center, Standford University, Standford, CA, 1978.

Hess CT, Michel J, Horton TR, Prichard HM, Coniglio, WA. The occurrence of radioactivity in public water supplies in the United States. Health Phys 48: 553-586; 1985.

http://www4.nau.edu/microanalysis/Microprobe/EDS-Detector.html

http://www.camplin.talktalk.net/Tastrak/TNotes/Chap6.htm

http://www.df.uba.ar/users/sgil/labo5_uba/recursos/Gamma_Detection_Canberra.htm

http://www.eia.gov/energy_in_brief/major_energy_sources_and_users.cfm

http://www.hps.org/publicinformation/ate/q817.html

http://hyperphysics.phy-astr.gsu.edu/hbase/quantum/compton.html

http://www.pas.rochester.edu/~AdvLab/6-Gamma/Lab06%20GammaSp.pdf

http://www.nucleonica.com/wiki/index.php?title=Help:Gamma_Spectrum_Generator

http://www.sprawls.org/ppmi2/RADIOACT/

http://world-nuclear.org/info/inf30.html

Ibrahim N. 1999. Natural activities of 238U, 232Th and 40K in building materials. J Environ Radioact 43:255–258; 1999.

ICRP. The 2007 Recommendations of the International Commission on Radiological Protection. ICRP Publication 103. Ann. ICRP 37 (2-4). 2007.

ICRP. Radiological protection against radon exposure, Draft Report. ICRP Publication XXX. 2012.

Johnston A, Martin P. Rapid analysis of Ra in waters by gamma ray spectrometry. Appl. Radiat. Isot. 48(5):631–638; 1997.

Khan K, Khan HM. Natural gamma-emitting radionuclides in Pakistani Portland cement. Appl Radiat Isot 54:861– 865; 2001.

Koler M, Niese S, Gleisberg B, Jenk U, Nindel K. Simultaneous determination of Ra and Th nuclides, 238U and 227Ac in uranium mining waters by gamma ray spectrometry. Appl. Radiat. Isot. 52:717–723; 2002.

Kovler K, Perevalov A, Levit A, Steiner V, Metzger L. Radon exhalation of cementitious materials made with coal fly ash: Part 2 – testing hardened cement – fly ash pastes. J Environ Radioactiv 82(3):335–50; 2005.

Knoll, G. Radiation detection and measurement. Danvers, MA: John Wiley & Sons, Inc. 2000.

Kumar V, Ramachandran TV, Prasad R. Natural radioactivity of Indian building materials and by-products. Appl Radiat Isot 51:93–96; 1999.

Lucas HF Jr. Ra-226 and Ra-228 in drinking water. Paper presented at the 27th Annual Meeting of the Health Physics Society, Las Vegas, Nevada. 1982.

Malanca A, Passina V, Dallara G. Radionuclide content of building materials and gamma-ray dose rates in dwellings of Rio-Grande Do-Norte Brazil. Radiat Protect Dosim 48:199 –203; 1993.

Markkanen M. Radiation Dose Assessments for Materials with Elevated Natural Radioactivity. Report STUK-B-STO 32, Radiation and Nuclear Safety Authority – STUK, 1995.

Mishra UC, Lalit BY, Ramachandran TV. Relative radiation hazards of coal based and nuclear power plants in India. In: Proceedings of Sixth International Congress of the International Radiation Protection Association (IRPA), 7–12 May 1980, vol. I, W. Berlin, W. Germany. 537–540; 1980.

Mollah AS, Ahmad GU, Hussain SR, Rahman MM. The natural radioactivity of some building materials used in Bangladesh. Health Phys 50:849–852; 1986.

Mustonen R, Pennanen M, Annanmäki M, Oksanen E. Enhanced Radioactivity of Building Materials. Final report of the contract No 96-ET-003 for the European Commission. Radiation and Nuclear Safety Authority – STUK, Finland;1997.

Nakaoka A, Fukushima M, Takagi S. Environmental effects of natural radionuclides from coal-fired power plants. Health Physics 47: 407-416; 1984.

National Council on Radiation Protection and Measurements. Ionizing Radiation Exposure of the Population of the United States: Recommendations on limits for exposure to ionizing radiation. Bethesda, Maryland: National Council on Radiation; NCRP Report No. 93; 1987.

National Research Council Committee to Assess Health Risks from Exposure to Low Levels of Ionizing Radiation, Health Risks from Exposure to Low Levels of Ionizing Radiation: BEIR VII Phase 2. The National Academies Press. Washington, DC.; 2006.

Papastefanou C, Charalambous S. On the radioactivity of fly ashes from coal power plants. Zeitschrift fur Naturforschung 34(a): 533-537; 1979.

Papastefanou C, Charalambous S. Hazards from radioactivity of fly ash from Greek coal power plants (CPP). In: Proceedings of the Fifth International Congress of the International Radiation Protection Association (IRPA), 9–14 March 1980, vol. III, Jerusalem, Israel:161–165;1980.

Papastefanou C. Escaping radioactivity from coal-fired power plants (CPPs) due to coal burning and the associated hazards: a review J Environmental Radioactivity 101:191-200; 2010.

Siotis I, Wrixon AD. Radiological consequences of the use of fly ash in building materials in Greece. Radiat Prot Dosim 7(1–4):41–4; 1984.

Ramadan AB, Hodhod OA, Youssef MA, Fouda SA. Characterization of Local Egyptian Iron Ores for Use in Radiation Shielding Concrete. Health Phys. 90(4):371-376; 2006.

Ryman JC, Eckerman KF. *ALGAMP - A Monte Carlo Radiation Transport Code for Calculating Specific Absorbed Fractions of Energy from Internal or External Photon Sources*, ORNL/TM-8377 (Oak Ridge National Laboratory, Oak Ridge, TN); 1993.

Sathish LA, Nagaraja K, Ramachandran TV. The spatial and volumetric variations of radon in Bangalore Metropolitan, India. Int J of the Phys Sciences. 18(6):4348-4360; 2011.

Stabin MG. Radiation Protection and dosimetry: An introduction into Health Physics. New York, New York: Springer Science+Business Media, LLC; 2007.

Stranden E. Assessment of the radiological impact of using fly ash in cement. Health Phys. 44(2):145-153; 1983.

Taylor-Lange SC, Stewart JG, Juenger MCG, Siegel JA. The contribution of fly ash toward indoor radon pollution from concrete. Building and Environment 56:276-282; 2012.

Tomczynska J, Blaton-Albicka K, Pensko J, Fugiel D. The Results of Measurements of the Natural Radionuclides in Coal Power Plants Wastes and Light Concrete Samples. Report-TB-APF 80. Radiation Protection Department, Institute of Nuclear Research, Swierk, Poland:9; 1980.

Tracy BL, Prantl FA. Radiological impact of coal-fired power generation. J Environmental Radioactivity 2:145–160; 1985.

Trevisi R, Risica S, D'Alessandro M, Paradiso D, Nuccetelli C. Natural radioactivity in buildingmaterials in the European Union: a database and an estimate of radiological significance. J Environmental Radioactivity 105: 11-20; 2012.

Turhan S, Parmaksiz A, Kose A, Yuksel A, Arikan IH, Yucel B. Radiological characteristics of pulverized fly ashes produced in Turkish coal-burning thermal power plants. Fuel 89: 3892–3900; 2010.

Van Dijk W, de Jong P. Determining the Rn-222 exhalation rate of building materials using liquid scintillation-counting. Health Phys 1991;61:501–9.

Ulbak K, Jonassen N, Baekmark K. Radon exhalation from samples of concrete with different porosities and fly ash additives. Radiat Prot Dosim 7(1–4):45–8; 1984.

United Nation Scientific Committee on the Effects of Atomic Radiation. Sources and effects of ionizing radiation. New York: United Nations Sales Publication E.00.IX.3; UNSCEAR 1993 Report to the General Assembly of the United Nations; 1993.

United Nation Scientific Committee on the Effects of Atomic Radiation. Report to general assembly atomic radiation, United Nations, New York: 2000.

United Nation Scientific Committee on the Effects of Atomic Radiation (UNSCEAR). Sources and effects of ionizing radiation, report to the general Assembly of the United Nations. New York: United Nations; 2008 [Annex B].

USGS. Radioactive elements in coal and fly ash: abundance, forms, and environmental significance. US Geo Surv Fact Sheet FS-163-97; 1997.

Vandenhove H. European sites contaminated by residues from the ore extracting and processing industries. p. 61-89 in: Restoration of Environments with Radioactive Residues. Proceedings Series. STI/PUB/1092. IAEA, Vienna; 2000.

Warner GG, A. M. Craig AM Jr. "ALGAM, A Computer Program for Estimating Internal Dose from Gamma-Ray Sources in a Nan Phantom", ORNL/TM-2250, Oak Ridge National Laboratory; 1968.

World Health Organization, WHO. Handbook on indoor radon: a public health perspective. France: WHO Library Cataloguing-in-Publication; 2009.

Xinwei L. Radioactive Analysis of Cement and Its Products Collected From Shaanxi, China. Health Phys 88(1):84–86; 2005.